Table 4-2-2 List of samples and seafloor photographs of LC sampling

Seamount	Sampling No.	Samples / Crust type	Exposed rate of crust	Crust type	Observation of seabottom
MS01	96SMS01LC01	Mud, F. sand, Bas py. rock	60 %	Nodule	Nodule, Boulder
	96SMS01LC02	F. sand, Ooze	0 %		Ripple mark
	96SMS01LC03	Crust	50 %	Crust	Botryoidal
	96SMS01LC04	Crust	5 %	Crust	Botryoidal
	96SMS01LC05	Crust	10 %	Crust	Botryoidal
	96SMS01LC06	(Void)	90 %	Crust	Botryoidal
	96SMS01LC11	Crust	10 %	Crust	Botryoidal
MS02	96SMS02LC01	Crust	20 %	Crust	Botryoidal
	96SMS02LC02	Pebble	20 %	Crust, Pebble	Botryoidal
	96SMS02LC03	(Void)	50 %	Crust	Botryoidal
	96SMS02LC04	Crust	80 %	Crust	Botryoidal
	96SMS02LC05	(Void)	50 %	Crust, Pebble	Botryoidal
	96SMS02LC06	Crust	30 %	Crust, Pebble	Botryoidal
MS03	96SMS03LC01	Crust	(Break down)		
	96SMS03LC02	F. sand	0 %		Ripple mark
	96SMS03LC03	F. sand	0 %		Ripple mark
	96SMS03LC04	(Void)	0 %		
	96SMS03LC05	Crust fragment	(Break down)		
	96SMS03LC06	(Void)	0 %		Ripple mark
MS04	96SMS04LC01	(Void)	90 %	Crust	Botryoidal
	96SMS04LC02	Crust	70 %	Crust	Botryoidal
	96SMS04LC03	Crust fragment	0 %		Ripple mark
	96SMS04LC10	F. sand	0 %		Ripple mark
MS05	96SMS05LC01	(Void)	80 %	Pebble	
	96SMS05LC02	F. sand	0 %		
	96SMS05LC03	(Void)	0 %		
	96SMS05LC04	(Void)	(Break down)		
MS06	96SMS06LC03	(Void)	30 %	Pebble	Botryoidal
	96SMS06LC04	(Void)	0 %		Ripple mark
	96SMS06LC05	F. sand, Sandy mudstone	0 %		Ripple mark
	96SMS06LC06	Crust fragment	30 %	Pebble	Botryoidal
MS08	96SMS08LC01	Crust	20 %	Crust	Botryoidal
	96SMS08LC02	Crust	20 %	Crust	Botryoidal
	96SMS08LC03	Crust	30 %	Crust	Botryoidal
	96SMS08LC11	Crust	(Break down)		
MS09	96SMS09LC01	Mud, Lappili tuff	30 %	Pebble, Nodule	
	96SMS09LC02	Crust fragment	(Break down)		
	96SMS09LC03	(Void)	60 %		Botryoidal
	96SMS09LC04	Crust	0 %		Ripple mark
	96SMS09LC05	F. sand, Crust	0 %		
	96SMS09LC06	Crust	10 %	Crust	Botryoidal

Legend F. sand : Foraminifera sand, Bas py. rock : Basaltic pyroclastic rock

96SMS03LC03

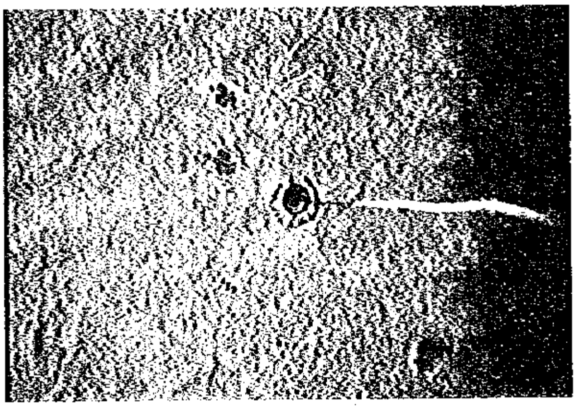

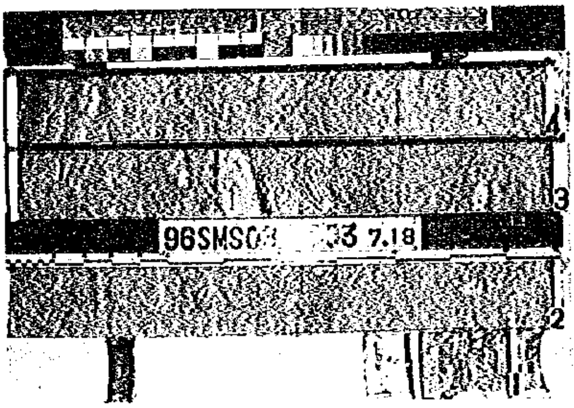

96SMS04LC10

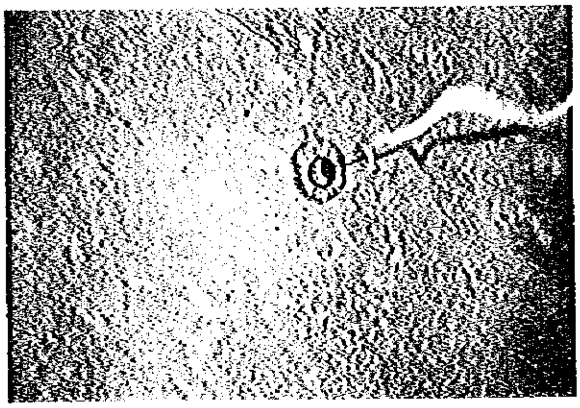

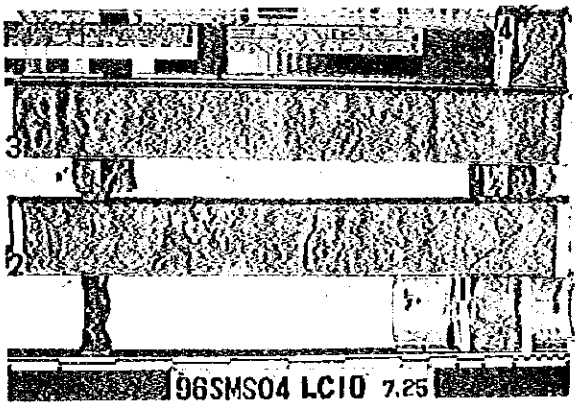

96SMS06LC05

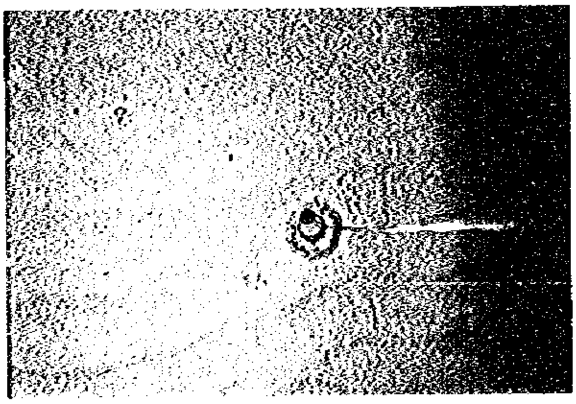

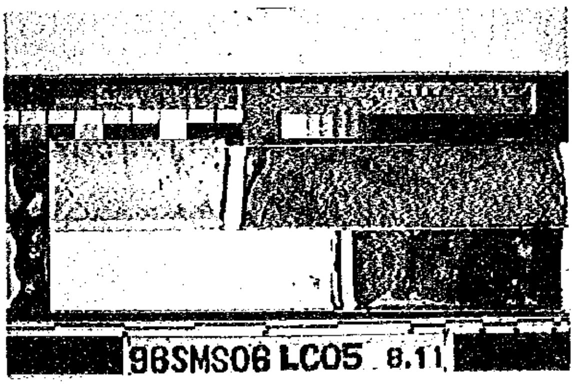

96SMS09LC01

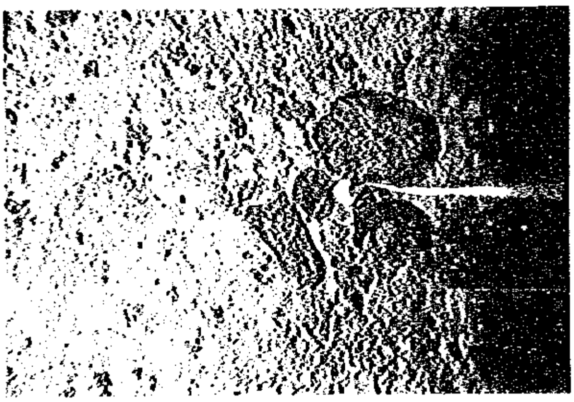

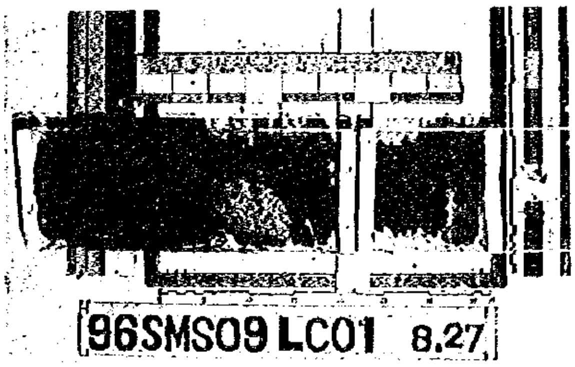

Note: In each site, upper photo shows a seafloor and lower a columnar section of core.

Fig. 4-2-3 Photographs of seafloor and sediments (LC sampling)

flank of seamounts, it was thought that only thick seafloor sediments would be collected, they were thinner, however, than anticipated and the underlying rocks were also collected. The seafloor sediments of the former are alternation of foraminifera sand and mud with some gravels, while the latter consist only of mud. On the other hand, 96SMS06LC05 and 96SMS09LC05 locate on the summit of guyots, and sampling objectives were manganese crusts, but foraminifera sand and rocks or manganese crusts were obtained. The seafloor photographs show only seafloor sediments for both localities.

Photographs of 96SMS09LC04 show only seafloor sediments on the seafloor, but sampling resulted in obtaining only manganese crust (see Fig. 5−3−2). This is believed to be the result of thin (under several 10 cm) seafloor sediments and they were washed away during lifting up the LC.

The nature of the collected samples is as follows.

1) 96SMS01LC01

The recovered core is 230cm long. Mud−dominant alternation with foraminifera sand extends down to 220 cm from the surface. Mud includes foraminifera fossils and rarely basalt pebbles (under 1cm). Many subrounded to subangular basalt pebbles attaining 6 cm occur in the foraminifera sand. Some of the pebbles are covered by manganese crusts with a maximum thickness of 5 mm. As this is located at the lower flank of the seamount (4,324 m deep), the pebbly foraminifera sand is believed to be a secondary deposit supplied from the upper flank. In the seafloor photograph nodules and float pebbles smaller than 5cm occupy 80% of the photo area and the amount of seafloor sediments is small.

Pale yellowish brown basaltic pyroclastic rock occurs bellow 220 cm depth. Lapilli are subangular basaltic pebbles less than 3 cm. The matrix is the same clastic materials as lapilli and argillized. This surface is not covered by manganese crusts.

2) 96SMS01LC02

The recovered core is 95 cm long. The core from the surface to 15 cm in depth consists of ooze with high water content. The core below 15 cm depth consists of foraminifera sand with intercalation of mud.

3) 96SMS03LC02

The recovered core is 105 cm long. The core from the surface to 15 cm in depth consists of ooze with high water content. The core below 15 cm depth consists of foraminifera sand which is nearly homogeneous and partly includes mud.

4) 96SMS03LC03 (Fig. 4-2-3)

The recovered core is 310 cm long. It consists of nearly homogeneous foraminifera sand with partial mud content and pebbles do not occur.

5) 96SMS04LC10 (Fig. 4-2-3)

The recovered core is 220 cm long. It consists of homogeneous foraminifera sand with partial mud content. It contains black foraminifera shells and pebbles do not occur.

6) 96SMS05LC02

The recovered core is 100 cm long. It consists of homogeneous foraminifera sand. No pebbles occur. Some parts are pale gray.

7) 96SMS06LC05 (Fig. 4-2-3)

The recovered core is 75 cm long. The core from the surface down to 65 cm in depth consists of homogeneous foraminifera sand without pebbles or mud. The core below 65 cm depth consists of dark reddish brown sandy mudstone. This surface is not covered by manganese crusts.

8) 96SMS09LC01 (Fig. 4-2-3)

The recovered core is 40 cm long. The core from the surface down to 15 cm in depth consists of dark brown ooze with small amount of fine sand. Seafloor photograph shows the predominance of seafloor sediments with cobble crusts and nodules occupying approximately 30%.

The core below 15cm depth consists of dark reddish brown basaltic lapilli tuff. Lapilli consists of brown subangular basalt pebbles less than 1cm and the yellowish brown matrix is argillized. Rock surfaces are covered by thin-coating to 10 mm thick manganese crusts.

9) 96SMS09LC05 (Fig. 5-3-2)

The recovered core is 60 cm long. The core from the surface down to 50 cm in depth consists of nearly homogeneous foraminifera sand, and mud is intercalated in the lower part.

Manganese crust occurs below 50cm depth and it is 4 cm thick. Substrate rocks were not collected.

(3) Summary by seamounts

Basalt and basaltic pyroclastic rocks were collected in all seamounts and they constitute the largest portion of the sampled material. They are the major substrate of the manganese crusts. The appearance of these rocks is very similar and there is no apparent difference among those of individual seamounts. Unique or typical examples are: basalt pillow lava at MS04 seamount (Fig. 4-2-2 (1), Photo Nos. 1, 2), basalt having a coarse grained porphyritic texture with many phenocrysts (Fig. 4-2-2 (1), Photo No. 4) and a non-porphyritic texture (Fig. 4-2-2 (1), Photo No. 3) at MS08 seamount. Pumice of unknown origin were collected at MS05 and MS07 seamounts. These two seamounts are both peaked seamounts while others surveyed are all guyots. Although the possibility of these pumice being autochthonous cannot be denied, they are fairly well rounded and are not covered by manganese crusts, so they are believed to be relatively young volcanic rocks transported by sea current.

Sandstone and limestone were the most abundant sedimentary rocks collected. The appearance of the sandstone, mudstone, and limestone varies considerably for each seamount and the sampling location. Volcanic conglomerate was characteristically found only at MS08 seamount. Phosphatization is generally observed at all seamounts, and phosphorite forms network veins filling the fissures of rocks and manganese crusts.

The nature of the rocks collected at each seamount are as follows.

1) MS01

Basaltic pyroclastics and breccia were the most abundantly collected in this seamount. Basalt, mudstone, limestone, and mud block were also collected. Basalt inclines to be dominant at the flat summit of seamount while pyroclastics and breccia predominate at the flanks. Mudstone is sandy with weak stratification and was collected at the lower flank together with weakly consolidated mud block. Limestone consists mainly of foraminifera and was collected at the upper flanks.

The core from 220 to 230cm (bottom) deep of 96SMS01LC01 located at the lower flank, below the seafloor sediments, consists of basaltic pyroclastic rock.

2) MS02

Large amount of basalt, basaltic breccia, basaltic pyroclastic rocks were collected together with limestone, sandstone, and mudstone. Volcanic rocks were entirely collected from the flat summit to the lower flank of seamount. There appears to be no correlation between the sampling locality and the volcanic rock type collected. Sandstone were collected at the marginal part of the flat summit and the upper flank, and limestone at the shoulder of the summit.

3) MS03

Basalt, sandstone, and limestone were mainly collected with small amount of basaltic pyroclastics and breccia. Some samples of basalt are green as the result of weak alteration. Sandstone is derived from limestone and was collected at the flat summit margin of the seamount. Limestone were collected at the marginal part of flat summit and the upper flank.

4) MS04

Basalt was the most abundant and fair amount of basaltic pyroclastic rocks and basaltic breccia were also collected. Sandstone and limestone were collected together. Volcanic rocks were collected from the entire flank of seamount, and there is no correlation between the rock type and the sampling locality. Basalt pillow lava was collected at the lower flank of the eastern side. Many of the sandstone were reddish brown and they were collected at the entire flank. Limestone were collected at the upper and lower flank.

5) MS05

Basalt was the most abundant and basaltic pyroclastic rocks, limestone, phosphorite, sandstone, and pumice were also collected. This is a peaked seamount and there is a tendency of volcanic rocks dominating at the upper flank of seamount while sedimentary rocks dominating at the lower flank. Pumice is of pebble size and very small amount was collected. Limestone was collected at the middle flank. Phosphorite, considered to be derived from limestone, was collected at the lower flank.

6) MS06

Many basalt and basaltic pyroclastics were collected together with some limestone, basalt breccia, mudstone, and phosphorite. Volcanic rocks tend to dominate at the flat summit of seamount and limestone at the upper flank.

The core from 65 to 75 cm deep (bottom) of 96SMS06LC05 located on the flat summit, underlying foraminifera sand, consists of dark red mudstone (Fig. 4−2−3).

7) MS07

Basalt and basaltic pyroclastics were collected at the central upper flank of the peaked seamount. Pumice and phosphorite were collected at the pinnacles in the southern part. Only one pumice with 15cm diameter was recovered. All phosphorite occur as nuclei of manganese nodules.

8) MS08

Basalt and basaltic pyroclastic rocks are the most abundant and fair amount of basalt breccia, volcanic conglomerate, and sandstone were also collected. Aside from above, limestone, phosphorite, and tuff were collected. Volcanic rocks tend to dominate at the flat summit of seamount while sedimentary rocks at the flank. Rounded basaltic pebbles are observed on the middle to lower flank. Volcanic conglomerate were collected at the flat summit margin and the lower flank. Although the above two localities are separated, the volcanic conglomerate collected from the two localities are essentially similar. Limestone were collected on the whole flank from the upper to the lower part. There are two types of sandstone, one is coarse grained sandstone containing basalt granules and the other is fine grained sandstone containing many foraminifera fossils. These sandstone tend to be collected at the upper flank. Weakly altered green tuff was collected at the margin of the flat summit.

9) MS09

Basalt, basaltic pyroclastic rocks, limestone, and phosphorite are abundant, and basalt breccia and mudstone were also collected. Basalt were collected at the flat summit and the upper flank of seamount while basaltic pyroclastics throughout the seamount. Many of the limestone are phosphatized and they were collected at the flank together with phosphorite. Mudstone is brown with thin bedding and it was collected at middle flank. Limestone and phosphorite were collected more on this seamount than on others.

The core from 15 to 40 cm deep (bottom) of 96SMS09LC01 located on the foot of seamount, underlying seafloor sediments, consists of reddish brown basalt lapilli tuff. This surface is covered by thin manganese crusts (Fig. 4-2-3).

4-3 Description of Rocks

(1) Microscopic observation of rock thin sections

Rocks collected by AD and LC samplings were prepared into thin sections and studied by a polarization-microscope. The largest parts of the collected rocks were basalt and basaltic pyroclastic rocks. The number of samples studied is 43, and 21 of these samples are examined by X-ray diffraction analysis mentioned after. The results of microscopic observation are shown in Tables 4-3-1 (1), (2), and representative microphotographs are laid out in Figures 4-3-1 (1), (2).

Almost all basalt are weathered and the matrix of the pyroclastic rocks are argillized through the unaided eyes. Many rocks have been phosphatized. Most of basalt are vesicular with many gas cavities and are magnetic.

The following rocks were identified and studied microscopically. Volcanic rocks; basalt, basaltic pyroclastic rocks, and quartz porphyry; sedimentary rocks; sandstone, mudstone, and phosphorite. Basalt is largely grouped into porphyritic basalt and aphyric basalt, and each basalt is further divided into vesicular type and compact type. Vesicular porphyritic basalt is predominant and the amount of aphyric and compact basalt is small.

The major and typical rocks are described below.

1) Basalt

a) Porphyritic basalt (clinopyroxene olivin basalt)

This basalt has porphyritic and intersertal texture, and is divided into vesicular type with many vesicles (96SMS04AD09−T1, 96SMS08AD04−T2), and non−vesicular compact type (96SMS04AD06−T1, 96SMS08AD15−T1).

The phenocrysts are olivine, clinopyroxene, and plagioclase. The phenocrysts are mostly 1 to 2 mm in size with a maximum of 4 mm. Olivine is granular or prismatic and generally is altered to iddingsite or clay minerals, but there are some fresh grains. Clinopyroxene is unaltered and has a zonal structure. Plagioclase is prismatic and is unaltered.

The groundmass has a intersertal texture and comprises micro−phenocrysts of iddingsite derived from olivine and clinopyroxene, prismatic plagioclase under 0.3 mm, and glass. The groundmass is devitrified and argillized. Plagioclase and clinopyroxene are not altered.

The vesicles are completely filled with colloform or amygdaloidal montmorillonite, zeolite, apatite and calcite, or the vesicle walls are thinly covered by these minerals.

b) Vitric porphyritic basalt (clinopyroxene olivine basalt)

This basalt is glassy with porphyritic texture and is vesicular. Samples of 96SMS02AD08−T1 and 96SMS08AD04−T2 are the type of this basalt.

The phenocrysts are olivine and clinopyroxene. The sizes of the phenocrysts are mostly 1 to 2 mm with a maximum of 4 mm. Olivine is granular and is completely altered to iddingsite, clay minerals, or carbonate minerals. Clinopyroxene is unaltered and has a zonal structure.

The groundmass is vitric and consists of micro−phenocrysts of olivine and clinopyroxene, and glass. Olivine is completely argillized or carbonatized. Clinopyroxene is unaltered. No prismatic plagioclase occurs. Glass is devitrified and argillized.
The conditions of the vesicles are the same as those of porphyritic basalt mentioned above.

c) Aphyric basalt

This basalt is aphyric and divided into vesicular type (96SMS02AD08−T2) and compact type without vesicles (96SMS01AD07−T1, 96SMS02AD14−T1).

There is very small amount of tiny phenocrysts, and the groundmass has a intersertal texture. The phenocrysts are completely replaced by clay minerals (montmorillonite and chlorite) and are inferred to be originally pyroxene from the external form. The groundmass consists of prismatic plagioclase under 0.3 mm, argillized mafic minerals (pyroxene?), minute opaque minerals, and glass. The glass is devitrified and argillized. Plagioclase is unaltered.

Table 4-3-1 (1) Results of microscopic observation for rock thin sections

Legend of amount
◎ : abundant ○ : moderate △ : a few • : rare

				Volcanic rocks																				Clastic rocks											
				Phenocrysts							Groundmass					Altered minerals								Fragments		Matrix									
Sampling point	Code	Rock name	Texture	Quartz	Plagioclase	Olivin	Hypersthene	Augite	Magnetite	Hematite	Glass	Plagioclase	Augite	Opaque minerals	Apatite	Sericite	Smectite	Saponite	Chlorite	Zeolite	Calcite	Tridymite	Albite	Rocks	Max. size (mm)	Quartz	Plagioclase	Glass	Augite	Calcite	Tridymite	Apatite	Biotite	Opaque minerals	Clay minerals
96SMS01AD07	T1	non-porphyritic basalt	intersertal		•						◎	◎		○	△	○			○				○												
96SMS01AD09	T1	tuffaceous mudstone																						basalt	0.3		△		•						○
96SMS01AD09	T2	basaltic lapilli tuff																	◎			○		basalt	0.5				•						◎
96SMS01AD11	T1	olivin augite basalt	intersertal		◎	(○)		•			◎	◎					○	△																	
96SMS02AD08	T1	augite basalt	hyaloophitic		△			○			◎	△		•	•		○	△			△														
96SMS02AD08	T2	non-porphyritic basalt	intersertal		△				△		○	◎		○			○		△																
96SMS02AD14	T1	non-porphyritic basalt	intersertal			(○)					△	◎	◎	○				△																	
96SMS02AD14	T2	basaltic lapilli tuff																△	◎	△		△		basalt			△	○							
96SMS02AD18	T1	quartz porphyry		△	○						○	○		○																					
96SMS03AD09	T1	calcic sandstone															○				◎			foraminifera	3.0					◎					
96SMS03AD10	T1	non-porphyritic basalt	intersertal		•			•	△		○	◎	○	○				○																	
96SMS04AD04	T1	basaltic lapilli tuff														•	◎	△		◎				basalt	3.0									○	◎
96SMS04AD06	T1	augite olivin basalt	intersertal			○		•			◎	◎	○	△				△																	
96SMS04AD09	T1	non-porphyritic basalt	intersertal		•						○	◎		◎			◎	○																	
96SMS04AD09	T2	tuffaceous mudstone															○					◎						◎						○	○
96SMS04AD11	T1	porous basalt	intersertal		○						◎	△		○			◎	○																	
96SMS04AD11	T2	porous basalt	intersertal		△				△		○						◎	○																	
96SMS04AD11	T3	basaltic lapilli tuff															◎	○	○					basalt	3.0		△	○						○	◎
96SMS04AD14	T1	basaltic lapilli tuff															◎	○		○	◎		○	basalt	5.0		△	○							◎
96SMS04AD14	T2	basaltic lapilli tuff															◎	○		○	○		○	basalt	20		○	○							◎
96SMS04AD15	T1	basalt	intersertal		△						◎	○					•	○			◎														
96SMS05AD06	T1	olivin augite basalt	hyaloophitic					◎	△		◎		○	○				◎		△															

Table 4-3-1(2) Results of microscopic observation for rock thin sections

Legend of amount ◎ : abundant ○ : moderate △ : a few · : rare

				Volcanic rocks																				Clastic rocks											
				Phenocrysts							Groundmass					Altered minerals								Fragments		Matrix									
Sampling point	Code	Rock name	Texture	Quartz	Plagioclase	Olivin	Hypersthene	Augite	Magnetite	Hematite	Glass	Plagioclase	Augite	Opaque minerals	Apatite	Sericite	Smectite	Saponite	Chlorite	Zeolite	Calcite	Tridymite	Albite	Rocks	Max. length (mm)	Quartz	Plagioclase	Glass	Augite	Calcite	Tridymite	Apatite	Biotite	Opaque minerals	Clay minerals
96SMS05AD06	T2	basaltic lapilli tuff															◎	○	△	△				basalt	5.0		△	◎						△	○
96SMS05AD13	T1	basaltic lapilli tuff															○	○						basalt	5.0		·	◎	○					·	○
96SMS06AD01	T1	basaltic volcanic breccia																						basalt	10		○	◎						○	○
96SMS06LC05	T1	tuffaceous mudstone															◎											○						◎	◎
96SMS06AD09	T1	basalt	hyaloophitic		◎			○	○		◎	◎	(○)				○	○	◎																
96SMS06AD09	T2	basaltic lapilli tuff															◎	◎						basalt	5.0		◎	◎	○					◎	◎
96SMS07AD01	T1	basaltic lapilli tuff															◎	△						basalt	20		△	◎						◎	
96SMS07AD02	T1	basaltic lapilli tuff															◎							basalt	3.0			◎						△	◎
96SMS07AD03	T1	basaltic volcanic breccia															△	△						basalt	7.0			◎						◎	○
96SMS08AD04	T1	non-porphyritic basalt	intersertal								◎	◎	○	○			△																		
96SMS08AD04	T2	non-porphyritic basalt	intersertal								○	◎	○	○	·		○			△	△														
96SMS08AD04	T3	basaltic tuff															◎	○			○	△		basalt	3.0		△	◎	○					○	◎
96SMS08AD05	T1	basaltic lapilli tuff															◎	○		○				basalt	5.0			◎	·			△		△	◎
96SMS08AD08	T1	coarse grained sandstone															○	○		○				basalt	5.0		○		◎					○	○
96SMS08AD12	T1	basaltic lapilli tuff															◎							basalt	2.0				◎			·		○	◎
96SMS08AD12	T2	basaltic lapilli tuff															◎	○			○	○		basalt	10			○	○			·		○	◎
96SMS08AD13	T1	sandy tuff															◎	○		△				basalt	0.2		○	◎	△				·	·	◎
96SMS08AD15	T1	olivin augite basalt	intersertal		○	(△)		○	△		○	◎	◎	○			○		○																
96SMS09AD08	T1	basaltic lapilli tuff															◎	○		·				basalt	3.0		△	◎						△	◎
96SMS09AD09	T1	augite basalt	hyaloophitic					◎			◎		○	△	△		○	○		△	○														
96SMS09AD11	T1	augite basalt	hyaloophitic					○			◎	○	○	○	△		◎	○			◎														

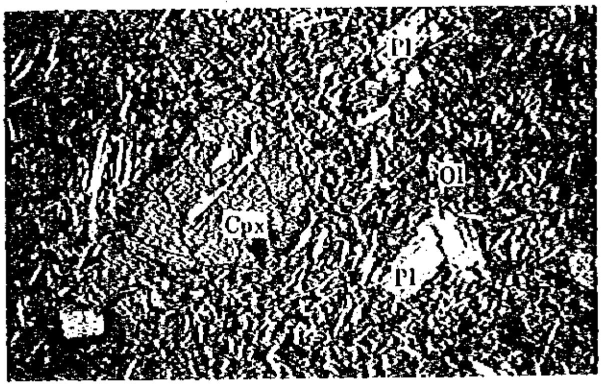

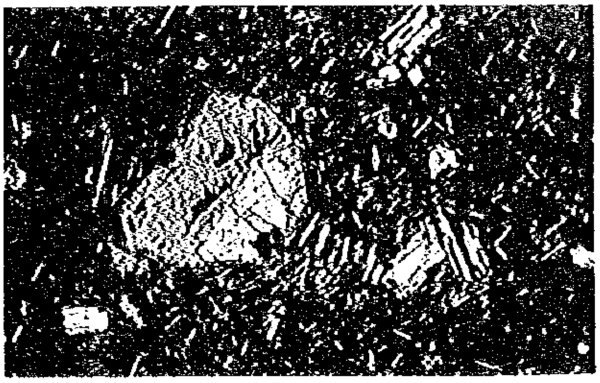

96SMS08AD15T1 Olivin augite basalt

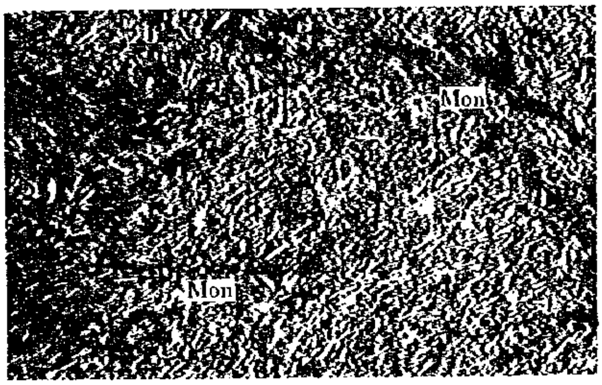

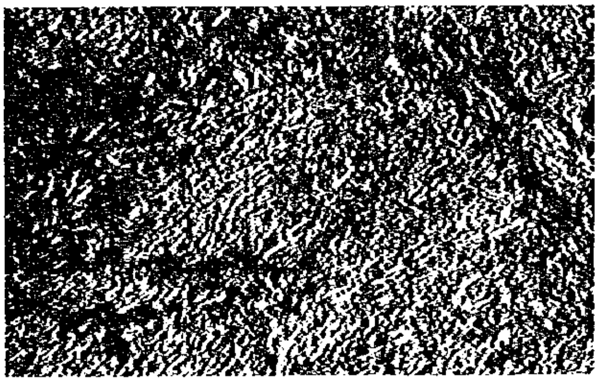

96SMS08AD04T1 Non-porphyritic basalt

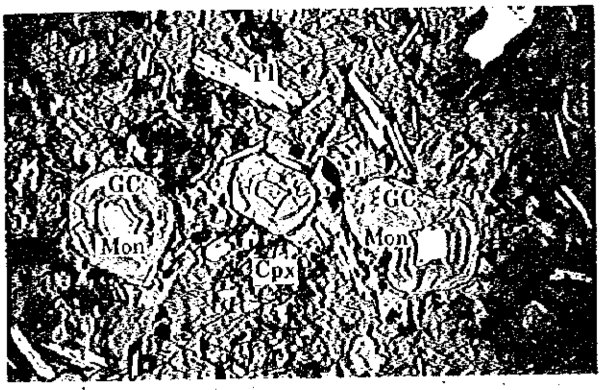

96SMS08AD15T1 Augite basalt (porous)

Note: Left side photos show open nicol, right side photos crossed nicols.
Legend is shown in next page.

Fig. 4-3-1(1) Photographs of microscopic observation of rock thin sections

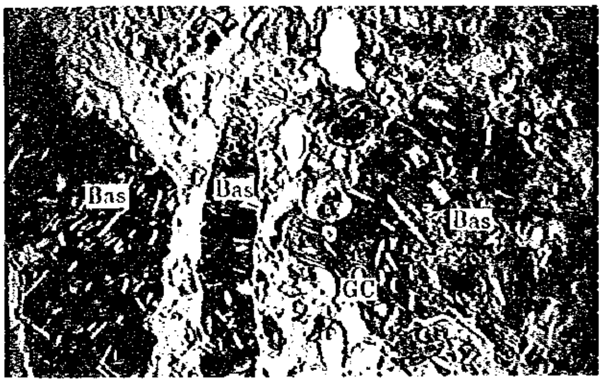

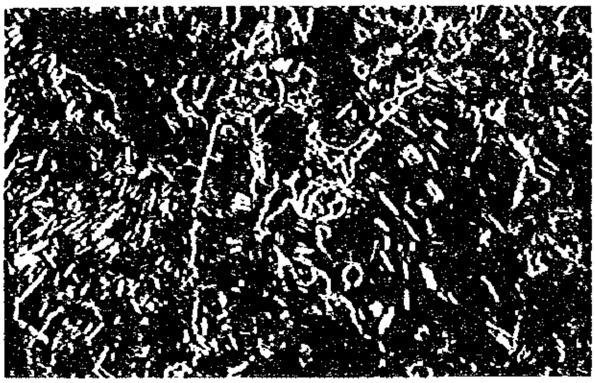

96SMS06AD09T2 Basaltic pyroclastic rocks

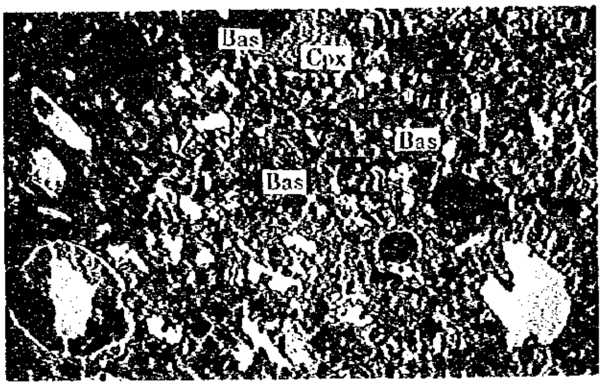

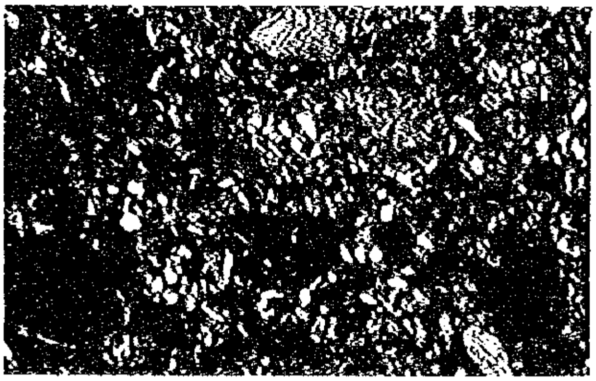

96SMS08AD08T1 Coarse grained sandstone

Note: Left side photos show open nicol, right side photos crossed nicols.

Legend Pl: plagioclase, Ol: olivin, Cpx: augite,
Mon: montmorillonite, Bas: basalt gravel, GC: gas cavity

Fig. 4-3-1 (2) Photographs of microscopic observation of rock thin sections

Vesicles are either completely filled with colloform montmorillonite, zeolite, and apatite, or the vesicle walls are thinly covered by these minerals.

2) Basaltic pyroclastic rocks

These are lapilli tuff and tuff breccia.

Lapilli of these rocks are all basalt fragments. The textures of the basalt do not differ from the various basalts mentioned above, but it is generally vesicular and aphyric.

The matrix consists of fine basalt fragments, mineral fragments, clay minerals, and microfossils of foraminifera, and the interstices are filled with colloform or amygdaloidal montmorillonite, zeolite, and apatite. These also occur around the outer margins of the lapilli. Mineral fragments are clinopyroxene and plagioclase, and are generally unaltered.

3) Quartz porphyry

The phenocrysts are small amount of quartz, plagioclase and alkali feldspars. Quartz is granular (under 1 mm diameter) and is corroded. The groundmass consists of fine-grained granular quartz, idiomorphic feldspar and glass. Glass is devitrified and weakly argillized. Some phenocrysts of plagioclase are partly argillized.

This rock is found only in one sample of 96SMS02AD18-T1, and is unusual considered from the geologic environment of the survey area.

4) Medium to coarse-grained tuffaceous sandstone

The clastics are consists of irregular basaltic fragments under 1cm and argillized fine fragments of basalt and clinopyroxene filling their interstices. The groundmass has no bedding and is composed of minute clay minerals, and the interstices are filled with montmorillonite, zeolite, and radial aggregation of apatite.

5) Tuffaceous mudstone

The clastics are consists of small fragments (under 0.3 mm) of volcanic glass, basalt, and plagioclase. Some of the volcanic glass show a fibrous texture and are often argillized. The matrix consists of minute clay minerals and is massive without bedding.

(2) X-ray diffraction analysis

X-ray diffraction analysis was carried out for collected rocks with the purpose of mainly identifying alteration minerals. The measurements were done by the non-orientation powder method. The number of samples is 24 and 21 samples of those are also studied microscopically. The results are shown in Table 4−3−2.

Identified alteration minerals are montmorillonite, chlorite/montmorillonite mixed−layer mineral, sericite, quartz, tridymite, phillipsite, apatite, calcite, siderite, hematite, and geothite. Major constituents are; montmorillonite, phillipsite, calcite, and apatite.

Montmorillonite is identified in almost all samples, and are abundant particularly in pyroclastic and sedimentary rocks. Chlorite/montmorillonite mixed−layer mineral is identified in nearly half of the samples studied, and occurs mostly in pyroclastic and sedimentary rocks. Sericite is found in three samples. In the microscopic observation, these clay minerals occur abundantly in vesicles and groundmass of basalt and in matrix of pyroclastic and sedimentary rocks.

Quartz is identified in one mudstone sample, and tridymite in one sandstone. They both occur together with clay minerals.

Phillipsite is identified in eight samples; relatively fine grained pyroclastic rocks, tuffaceous sandstone, and white phosphatized rock. It tends to occur together with montmorillonite, but not with limestone and apatite.

Apatite is identified in half of the samples, and is abundant particularly in pyroclastic rocks. In the microscopic observation, apatite occurs to fill vesicles of basalt or to form narrow veins, and occurs abundantly in matrix of pyroclastic and sedimentary rocks.

Calcite is identified in eight samples. It is found in various rocks and tends to occur together with apatite. Siderite is found in one sample.

Hematite is identified in eight samples, sedimentary rocks and basalt. Goethite is found in one sample.

Table 4-3-2 Results of X-ray diffraction analysis for rocks

Sampling point	Code	Sample contents	Mon	M/C	Serp	Pl	Kf	Ab	Qz	Tri	Cpx	Amp	Phi	Cal	Sid	Apa	Goe	Hem	Ana	Others
96SMS02AD08	X1	Altered basalt	○				△									·			·	
96SMS02AD14	X1	White materials	·	·			·						◎	△						
96SMS04AD04	X3	Hyaloclastite	△	·			△						○							
96SMS04AD09	X1	Mudstone	○				△		△?							△		·		
96SMS05AD13	X1	Basaltic lapilli tuff	△											·		○				
96SMS05AD13	X2	Phosphorite												△		◎				
96SMS06LC05	X1	Mudstone	△	?			△							·		○		·		
96SMS06AD09	X1	Basalt	·			◎					○							·		Ilm: ·
96SMS06AD09	X2	Basaltic lapilli tuff	△			◎														
96SMS07AD01	X2	Phosphorite	○				△						◎			△		·		
96SMS07AD02	X1	Hyaloclastite	○																	
96SMS07AD03	X1	Basaltic lapilli tuff	·	·										△		◎				
96SMS08AD04	X1	Basalt				△	?	○			○					△	?			Mus: ·
96SMS08AD04	X2	Basalt	·		·?	◎					○	·?		○				·		
96SMS08AD04	X3	Tuff		○		△				·?				○	△?			·		
96SMS08AD05	X1	Basaltic lapilli tuff	·										△	△		○				
96SMS08AD08	X1	Sandstone	·				△				△		◎							
96SMS08AD12	X1	Hyaloclastite	△	·												○				
96SMS08AD12	X2	Basaltic lapilli tuff	○	·							△					△				
96SMS08AD13	X1	Tuff	△	△		△							○							
96SMS08AD15	X1	Basalt				◎				·?	○						·?			Mus: ·
96SMS09AD08	X2	Hyaloclastite	△	·		△					·		△							
96SMS09AD09	X1	Basalt	·								○		·					·		
96SMS09AD11	X3	Basalt	·	·							○					·		·		

Legend Amount ◎ : abundant, ○ : moderate, △ : a few, · : rare

Mon: Montmorillonite, M/C: Montmorillonite-Chlorite mixed layer mineral, Serp: Serpentine, Pl: Plagioclase, Kf: K-feldspar, Ab: Albite, Qz: Quartz, Tri: Tridymite, Cpx: Clinopyroxene, Amp: Amphibole, Phi: Phillipsite, Cal: Calcite, Sid: Siderite, Apa: Apatite, Goe: Goethite, Hem: Hematite, Ana: Anatase, Ilm: Ilmenite, Mus: Muscovite

4-4 Chemical Composition of Rocks

Chemical analysis was carried out for twelve basalt samples collected by AD. The analytical results are shown in Table 4-4-1.

(1) Analytical methods

Analytical methods used and elements analyzed are as follows. Before the sample preparation, samples were washed and dried until constant weight was confirmed.

* ICP emission spectrometry: SiO_2, TiO_2, Ai_2O_3, MnO, MgO, CaO, Na_2O, K_2O, P_2O_5, Rb, Sr, Ba, Zr, V, Nb, Y
* Neutralization titration: FeO
* Combustion and infrared absorption spectrometry (LECO): CO_2
* Gravimetry: H_2O+, H_2O-, LOI
* Neutron activation: La, Ce, Pr, Nd, Sm, Eu, Gd, Tb, Dy, Ho, Er, Tm, Yb, Lu

(2) Analytical results

The major contents vary considerably by sample. This is caused by the diverse lithology and texture of the basalts. The chemical trends of the various lithological features are as follows.

* Samples with compact and intersertal texture (96SMS01AD07-CA1, 96SMS03AD10-CA1, etc.) have high SiO_2, Al_2O_3, Na_2O contents.
* Samples with vitric and porphyritic texture (96SMS05AD06-CA1, 96SMS09AD09-CA1, 96SMS09AD11-CA1) have low SiO_2, Al_2O_3, Na_2O and high CaO contents.
* Samples with porphyritic texture containing olivine (96SMS04AD06-CA1,96SMS09AD09-CA1, 96SMS09AD11-CA1) have high MgO and FeO contents.
* 96SMS05AD06-CA1 which has very high CO_2 and LOI content is strongly argillized.

Table 4-4-1 Results of chemical analysis for rocks

Sampling point No.	Code	SiO2 (%)	TiO2 (%)	Al2O3 (%)	Fe2O3 (%)	FeO (%)	MnO (%)	MgO (%)	CaO (%)	Na2O (%)	K2O (%)	P2O5 (%)	C02 (%)	H2O+ (%)	H2O- (%)	LOI (%)	TOTAL (%)	Total Fe (%)	Mg #
96SMS01AD07	CA1	47.77	1.76	17.15	9.74	1.3	0.16	1.09	4.97	4.07	2.31	1.23	0.15	2.50	4.60	7.18	98.73	11.04	0.394
96SMS02AD16	CA1	34.95	5.12	11.98	10.22	5.7	0.20	6.81	11.58	1.13	0.78	1.29	0.14	3.58	5.62	9.09	98.88	15.92	0.481
96SMS03AD10	CA1	48.57	2.98	15.46	10.74	0.6	0.13	1.91	6.11	4.31	2.67	1.43	0.06	1.70	2.79	4.39	99.27	11.34	0.712
96SMS04AD06	CA1	42.93	2.23	13.87	8.51	5.0	0.19	9.44	12.05	2.28	0.88	0.40	0.46	1.28	1.21	2.67	100.41	13.51	0.594
96SMS04AD09	CA1	44.19	3.27	16.17	12.19	2.1	0.14	2.23	7.55	3.11	1.68	1.79	0.29	2.72	1.70	4.86	99.30	14.29	0.452
96SMS05AD06	CA1	35.89	2.56	12.32	7.96	3.1	0.16	4.69	17.33	1.15	1.39	1.10	7.05	3.57	1.85	10.24	97.89	11.06	0.540
96SMS06AD09	CA1	48.05	3.05	16.79	6.33	3.5	0.10	3.08	9.87	3.57	1.16	1.33	0.35	1.51	1.58	2.52	99.36	9.83	0.406
96SMS06AD13	CA1	37.91	4.07	15.77	11.40	3.0	0.19	2.95	10.60	2.24	1.46	3.84	0.44	3.46	1.87	6.29	99.76	14.40	0.433
96SMS08AD04	CA1	45.42	2.65	17.93	8.95	2.0	0.19	3.61	9.63	5.58	1.75	0.95	0.01	0.87	0.75	1.48	100.14	10.95	0.583
96SMS08AD15	CA1	47.05	3.19	17.87	7.57	2.7	0.17	4.08	8.99	4.87	1.66	0.65	<0.003	1.30	0.76	1.91	100.66	10.27	0.540
96SMS09AD09	CA1	38.66	3.76	12.76	7.69	6.3	0.16	9.86	10.85	1.82	1.43	0.60	0.55	3.48	2.62	6.16	100.03	13.99	0.548
96SMS09AD11	CA1	38.26	3.11	12.30	9.43	3.2	0.19	10.14	12.21	1.70	1.26	1.18	0.01	4.33	1.77	6.65	99.64	12.63	0.711

(3) Classification of basalt

The following diagrams were prepared from the major and minor elements' contents and the basalts were classified.

1) AFM diagram (Fig. 4−4−1)

Two samples, 96SMS08AD15−CA1 and 96SMS08AD15−CA1, are classified into calc−alkali rock series and the other 10 samples into tholeite series, but the plots are scattered as a whole. The plots for three samples containing olivine phenocrysts (96SMS04AD06−CA1, 96SMS09AD09−CA1, 96SMS09AD11−CA1) are closer to MgO end member.

2) $MnO-TiO_2-P_2O_5$ diagram (Fig. 4−4−2)

All 12 samples belong to the oceanic island alkali basalt (OIA). This is harmonious with the fact that the Marshall Islands are oceanic islands.

3) Zr−Nb−Y diagram (Fig. 4−4−3)

All 12 samples belong to the within plate alkaline basalt (WPA). This is harmonious with the fact that the Marshall Islands grew by hot spot activity.

4) REE chondrite normalized diagram (Fig. 4−4−4)

All 12 samples show declining linear normalized patterns rich in light REE, and this pattern is the same as that of oceanic island basalt. As there is a spread in the light REE contents compared to the heavy REE, the gradient of the pattern differs by sample. The gradient of 96SMS05AD06−CA1 and 96SMS09AD09−CA1 is the steepest, and 96SMS04AD06−CA1 and 96SMS04AD09−CA1 the gentlest. This variation of the gradient is considered to be simple unevenness and not caused by the lithology and texture of basalt or the location of the seamounts.

4−5 Age of Rocks

Rock age was determined by K−Ar dating method for eight basalt samples. Seven of these samples were analyzed chemically. The results of dating rocks are shown in Table 4−5−1.

Potassium was quantified by flame spectrometry and argon isotope ratio by rare gas mass spectrometry. Steiger and Jagers (1977) radioactive disintegration constant was used.

Seven samples show from Late Cretaceous to Paleogene age. This is harmonious with the fact that previous works indicate Cretaceous age for the seamounts in the vicinity of the Marshall Islands. There is

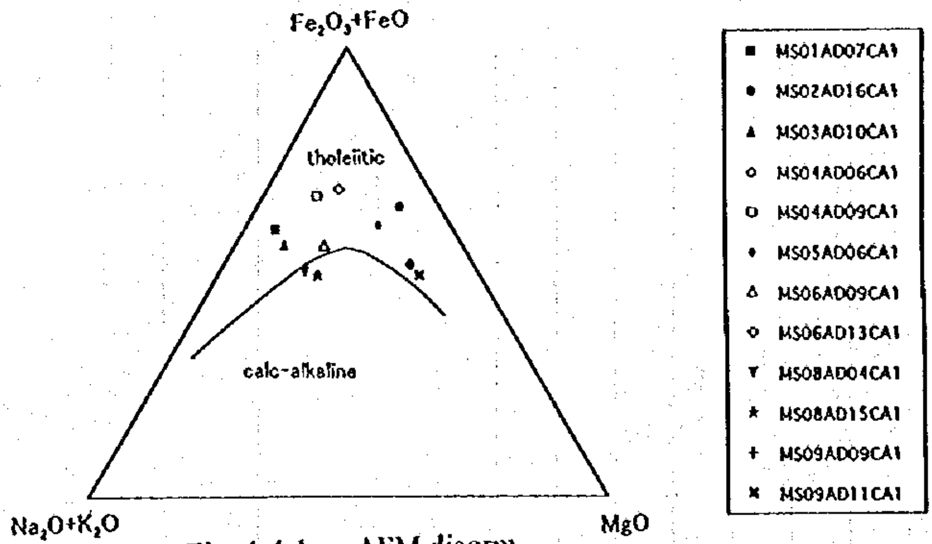

Fig. 4-4-1 AFM diagrm

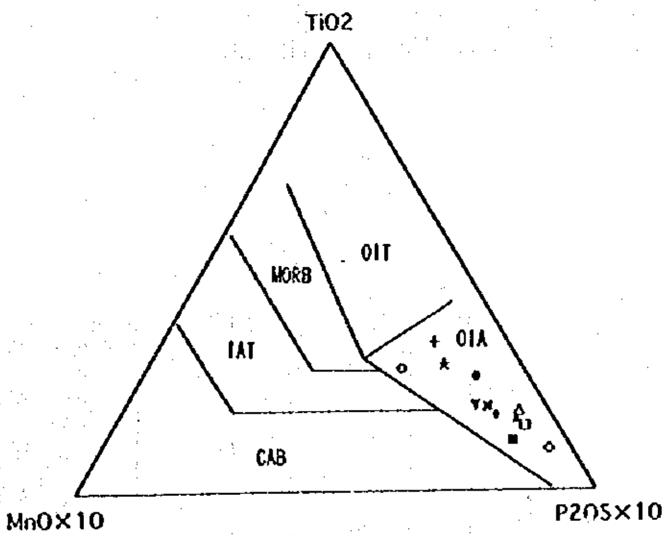

Fig. 4-4-2 Mn-TiO2-P205 diagram

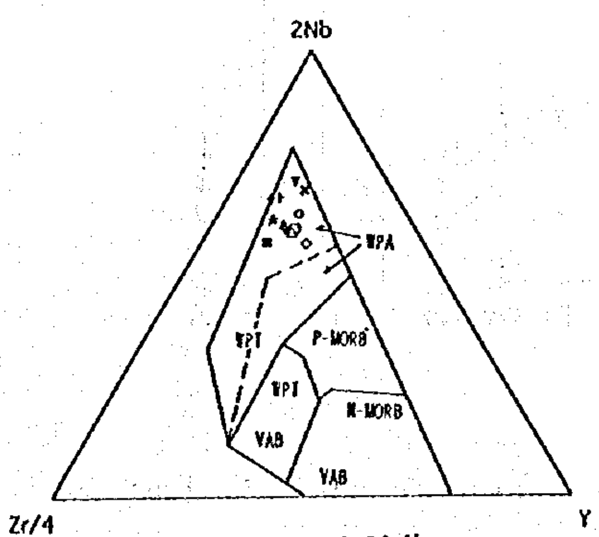

Fig. 4-4-3 Zr-Nb-Y diagram

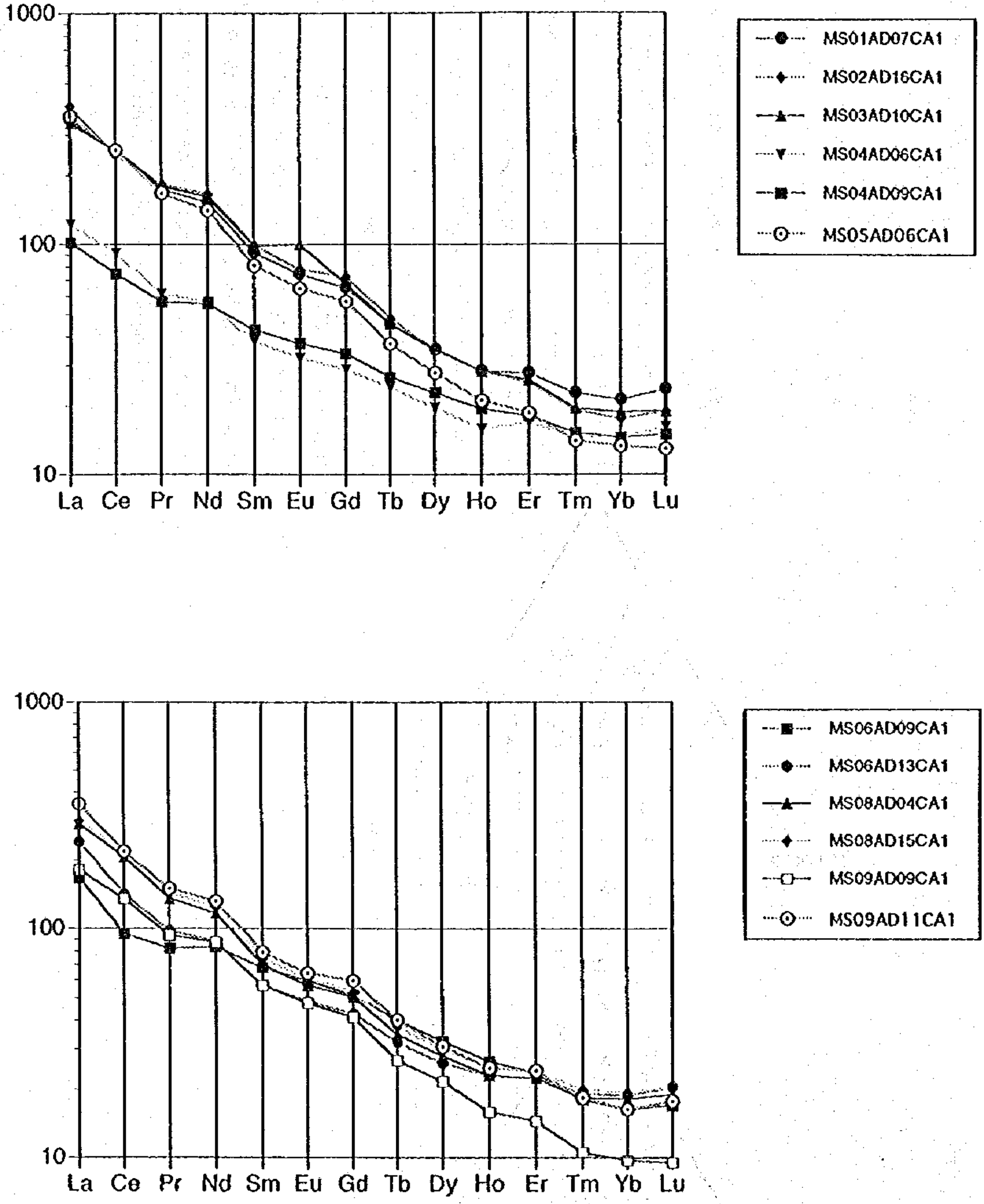

Fig. 4-4-4 REE normalized pattern diagram to chondrite

Table 4-5-1 Results of dating rocks

Sampling point No.	Code	Kalium (wt%)	Rad. 40Ar (nL/g)	Air contam. (%)	K-Ar age (Ma)	Alteraion grade (observation item)
96SMS02AD08	K1	1.19±0.01	2.64±0.04	31±1	56±1	Medium (thin section)
96SMS04AD09	K1	1.52±0.01	2.90±0.04	62±1	48±1	Medium (thin section)
96SMS05AD06	K1	1.20±0.01	1.63±0.02	50±1	35±1	Medium (thin section)
96SMS06AD09	K1	0.95±0.01	2.27±0.03	38±1	60±1	Medium (thin section, X-ray)
96SMS08AD04	K1	1.58±0.01	4.50±0.07	11±1	72±1	Weak (thin section, X-ray)
96SMS08AD15	K1	1.45±0.01	4.17±0.06	11±1	73±1	Weak (thin section, X-ray)
96SMS09AD09	K1	1.22±0.01	2.70±0.04	23±1	56±3	Medium (thin section, X-ray)
96SMS09AD11	K1	0.90±0.01	0.38±0.01	89±1	11±2	Medium (thin section, X-ray)

40K Decay Constants $\lambda e = 0.581 \times 10$ ^-10/year, $\lambda \beta = 4.962 \times 10$ ^-10/year

40K/K=0.01167 atm%

Table 4-6-1 Results of lead isotope analysis for rocks

Sampling point No.	Code	Sample	206Pb/204Pb	207Pb/204Pb	208Pb/204Pb
96SMS02AD08	IS1	Basalt	18.312	15.641	38.826
96SMS04AD09	IS1	Basalt	19.384	15.640	39.063
96SMS05AD06	IS1	Basalt	20.228	15.662	40.034
96SMS06AD09	IS1	Basalt	20.240	15.678	39.544
96SMS08AD04	IS1	Basalt	20.538	15.699	39.802
96SMS08AD15	IS1	Basalt	21.042	15.739	40.403
96SMS09AD09	IS1	Basalt	19.091	15.594	40.325
96SMS09AD11	IS1	Basalt	19.668	15.520	38.654

no clear relation with the location of the seamounts and these rock ages.

As shown in Table 4-5-1, all eight samples are studied by microscopic observation or X-ray diffraction analysis. These results show that all samples are generally argillized, carbonatized or phosphatized.

4-6 Lead Isotopic Composition of Rocks

Lead isotopic composition was determined for the same eight basalt samples as rock age was determined. The analytical results are shown in Table 4-6-1, and two-component diagrams of the lead isotope ratio in Figure 4-6-1.

(1) Analytical methods

Samples were treated with acid in order to expel sea water and were dried, and then lead was extracted and separated by Shimoda and Nohda method (1995).

Finnigan Mat mass spectrometer was used for determining the lead isotope ratio. Three isotope ratios determined are 206Pb/204Pb, 207Pb/204Pb, and 208Pb/204Pb. Correction factors for these measurements are 1.00290, 1.00425, and 1.00628 respectively.

(2) Analytical results

The three lead isotope ratios differ considerably by samples, and they are plotted in a wide region on the diagram of Figure 4-6-1. In the 208Pb/204Pb vs 206Pb/204Pb diagram, only 96SMS09AD09 is plotted significantly off the oceanic mantle area, and this is believed to be influenced by the sea water or the seafloor sediments. Plots of other samples lie within the oceanic island basalt.

The plot for 96SMS08AD15 lies near HIMU (high μ : high U/Pb ratio), and 96SMS08AD04, 96SMS05AD06, and 96SMS06AD09 also are plotted in the vicinity. Thus, it is considered that these four samples were derived from a magma with high HIMU component. On the other hand, three samples 96SMS02AD08, 96SMS04AD09, and 96SMS09AD11 are not affected by HIMU, and they are believed to have been derived from a different magma. The HIMU area is where 206Pb/204Pb is above 21.3 and 208Pb/204Pb is between 40.2 and 40.9 (Staudiget et al., 1991).

As above, the basalts of three seamounts, MS05, MS06, and MS08, and those of MS02, MS04, and MS09 are inferred to be of the different origin magmas. The former three seamounts are located in

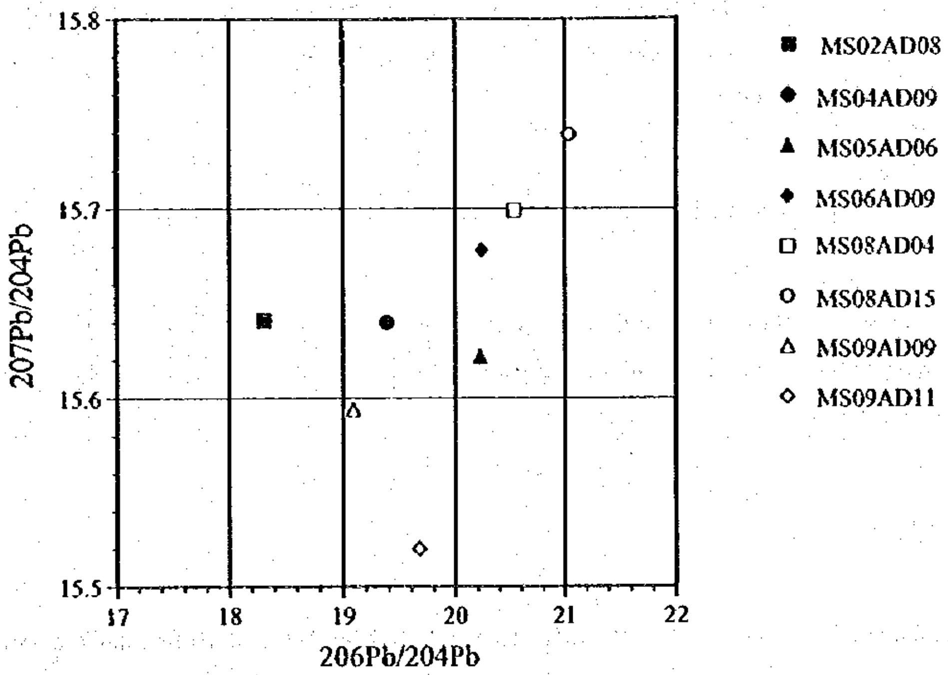

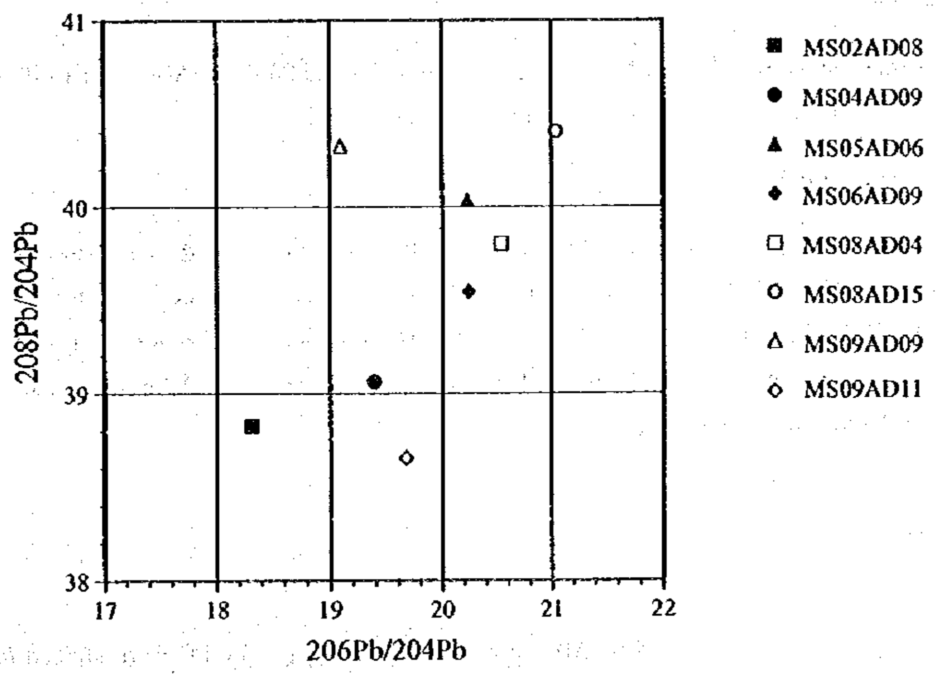

Fig. 4-6-1 208Pb/204Pb-206Pb/204Pb and 207Pb/204Pb-206Pb/204Pb diagram the southeastern part of the survey area, while the latter ones in the northwestern part, and it appears to have areal difference. The border of these two groups, however, crosses over the direction of the alignment of the seamounts (NNW–SSE), and it is difficult to explain the difference of origin magma by the location of seamounts.

4–7 Fossils in Rocks and Seafloor Sediments

Foraminifera, radiolaria, and coral fossils in limestone, mudstone and foraminifera sand collected by AD and LC were determined. The results are shown in Table 4–7–1 and the typical photomicrographs in Figures 4–7–1 (1), (2).

(1) Foraminifera

Foraminifera fossils of four limestone samples collected by AD, and 10 foraminifera sand samples, one mud sample and one mudstone sample collected by LC were determined. Foraminifera was not found in two limestone samples, one each of mudstone and mud samples.

1) Limestone

The sample 96SMS02AD15–F1 is correlated to Blow P9 and 96SMS09AD09–F1 to Blow P11, they are of Early Eocene and Middle Eocene Epochs respectively.

2) Foraminifera sand

All samples collected from cores shallower than 105 cm are correlated to Pleistocene Epoch. The sample 96SMS04LC10–F1 from 210 to 220 cm depth is correlated to Latest Pliocene, and 96SMS03LC03–F1 from 300 to 310 cm is to Latest Miocene. The absolute ages inferred in these samples are shown in Table 4–7–1. There is the relation even in different seamounts that the deeper depth shows the older age.

(2) Radiolaria

Four limestone samples collected by AD and one mudstone sample by LC were studied for radiolaria fossils.

Several radiolaria fossils were found in one limestone sample 96SMS02AD13–F1, but none occurs in other four samples. As the identified fossils are useless for age determination, it is impossible to obtain bioage from this sample.

Table 4-7-1 Results of fossil observation for rocks and seafloor sediments

Sampling point No.	Code No.	Depth (cm)	Sample	Geological time	
				Foraminifera	Radiolaria
96SMS01LC01	F1	0-5	Foraminifera sand	Pleistocene [650-220]	
96SMS01LC01	F2	42-47	Foraminifera sand	Pleistocene [650-220]	
96SMS01LC01	F3	80-85	Foraminifera sand	Pleistocene [650-220]	
96SMS01LC01	F4	220-230	Foraminifera sand	Barren	
96SMS01LC02	F1	45-50	Foraminifera sand	Pleistocene [300-120]	
96SMS01LC02	F2	85-90	Mud	Pleistocene [>300]	
96SMS02AD07	F1		Limestone (Calcite)	Barren	Unknown (No produce)
96SMS02AD13	F1		Limestone (Marble)	Barren	Unknown
96SMS03LC02	F1	100-105	Foraminifera sand	Pleistocene [650-220]	
96SMS03LC03	F1	300-310	Foraminifera sand	Latest Miocene	
96SMS04LC10	F1	210-220	Foraminifera sand	Latest Pliocene	
96SMS04AD15	F1		Limestone	Early Eocene (Blow P9)	Unknown (No produce)
96SMS05LC02	F1	100-105	Foraminifera sand	Pleistocene [300-120]	
96SMS06LC05	F1	60-65	Foraminifera sand	Pleistocene [>220]	
96SMS06LC05	F2	70-75	Mudstone	Barren	Unknown (No produce)
96SMS09AD09	F1		Limestone	Middle Eocene (Blow P11)	Unknown (No produce)

Notice:In Geologic time - Foraminifera column, the figures of [ ] indicates absolute age (unit:thousand years).

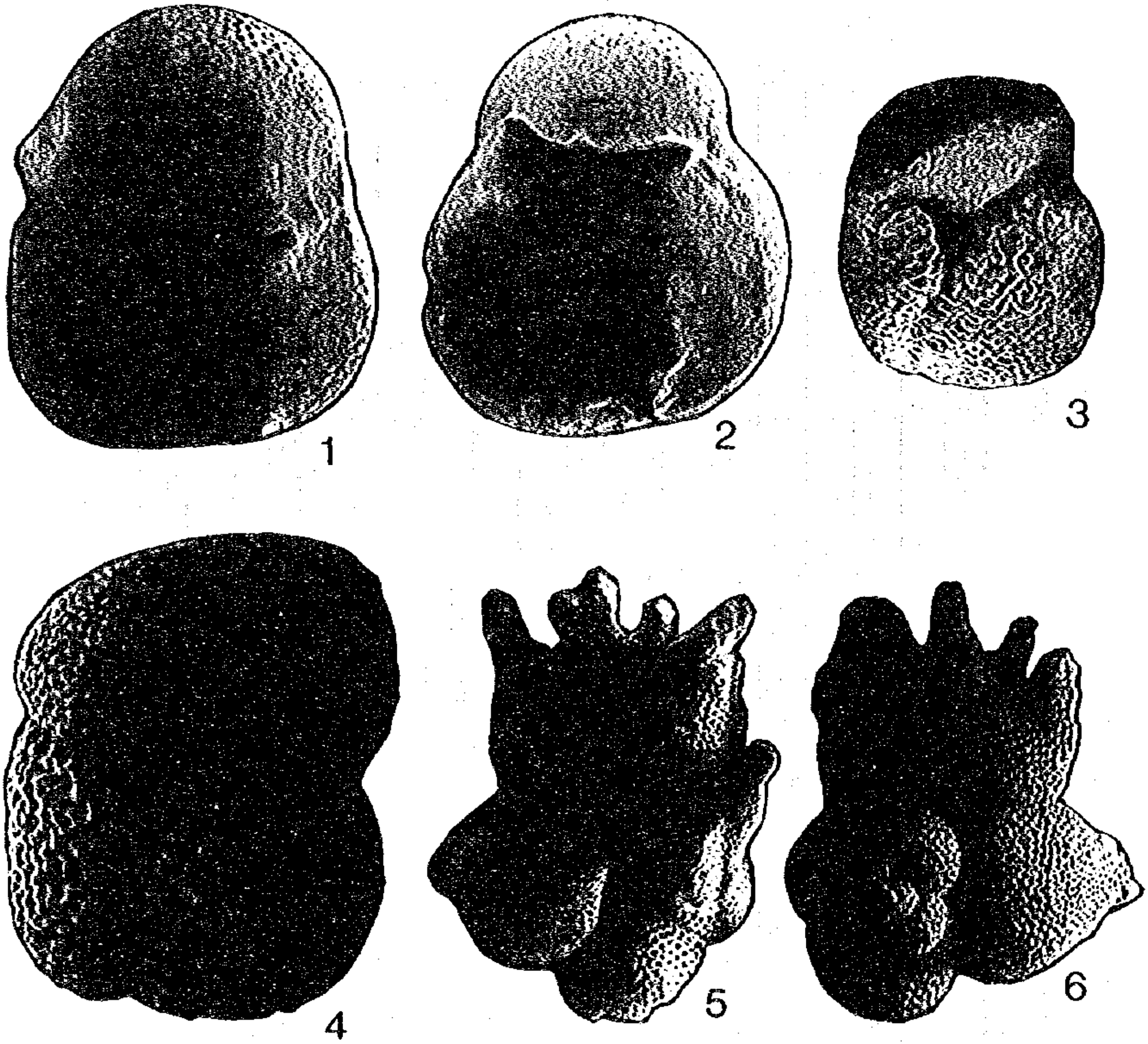

1, 2 Sphaeroidinella dehiscens (Parker and Jones)
Umbilical and spiral views, X 88, Pleistocene
Sample: MS01 LC01F2, 42-47 cm

3, 4 Globoquadrina dehiscens (Chapman, Parr and Collins)
Umbilical view, X 83 and spiral view, X 132
Latest Miocene. Sample MS03 LC03F1, 300-310 cm

5, 6 Globigerinoides fistulosus (Schubert)
Umbilical and spiral views, X 66; Pliocene
Sample: MS04 LC10F1, 210-220 cm

Fig. 4-7-1(1) Photographs of microscopic observation of microfossils

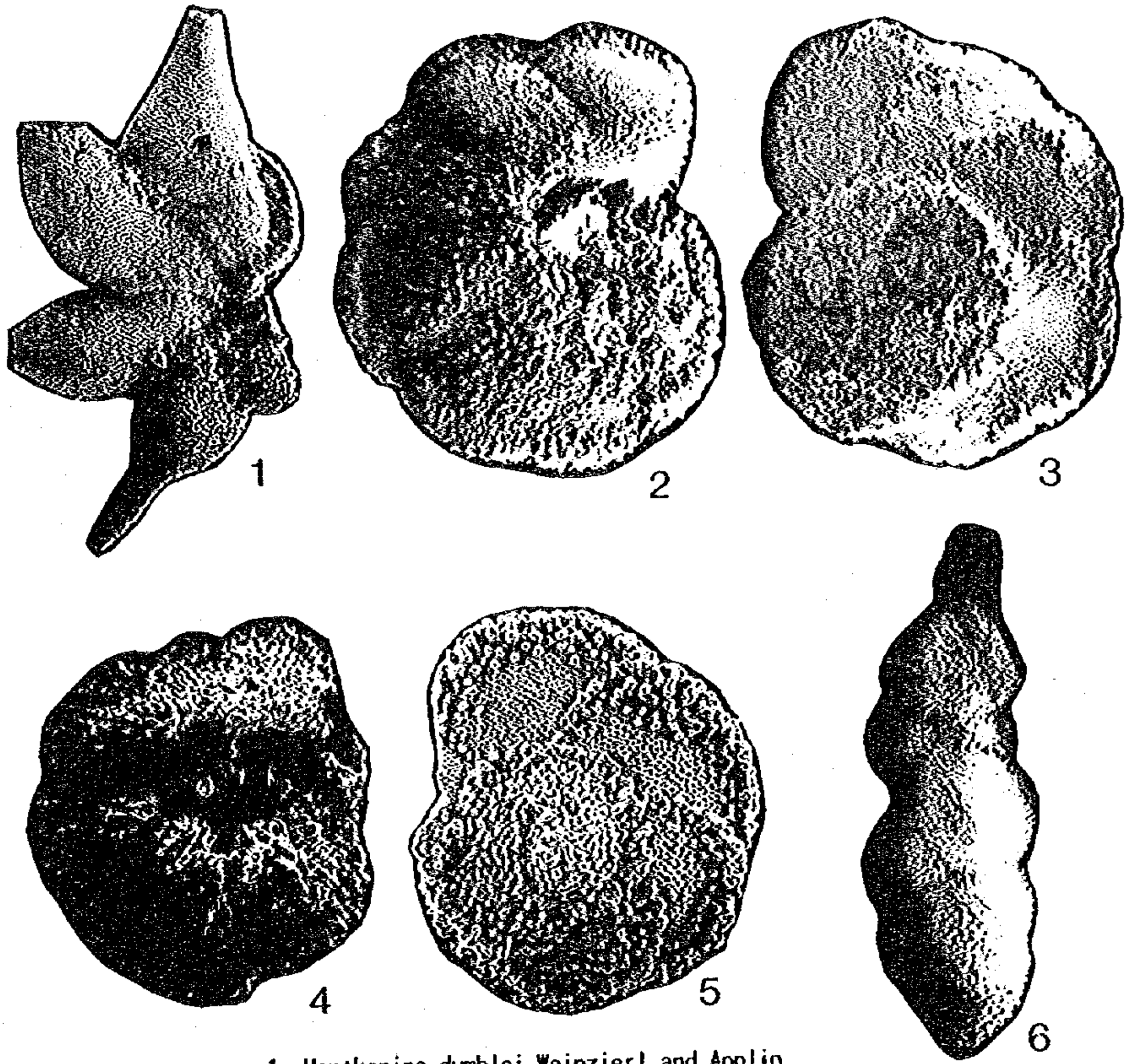

1 Hantkenina dumblei Weinzierl and Applin
Side view, X 88, Middle Eocene
Sample: MS09 AD09 F1

2, 3 Morozovella aragonensis (Nuttall)
Umbilical and spiral views, X 88; Middle Eocene
Sample: MS09 AD09 F1

4, 5 Morozovella acuta (Toulmin)
Umbilical and spiral views, X 123
Earliest Eocene. Sample: MSJ03 AD 23

6 Uvigerina proboscidea Schwager (底生有孔虫)
Side view, X 86
Sample: MS01 LC01F2, 42-47 cm

Fig. 4-7-1(2) Photographs of microscopic observation of microfossils

(3) Corals

The five samples used for radiolaria examination were also studied for coral fossils.

Hexacorallia fossils of Late Permian to Early Cretaceous were found in one limestone sample 96SMS02AD13−F1. Coral and shell fossils were not found in other four samples.

Chapter 5 Manganese Crusts

5−1 Classification and Layered Structure of Manganese Crusts

(1) Classification of manganese crusts by form

Manganese crusts are classified as follows in this report by the form of manganese crusts and substrate rocks. See Figures 5−3−1 (1), (2) which are the photographs of typical manganese crusts collected.

1) Crust (Fig. 5−3−1(1), Photo Nos. 5 to 8)

Crust is defined here as; an upper surface of sample is covered by manganese oxides and the substrate is exposed on the bottom surface.

There are two modes of occurrence of the crust; one forms directly on the substrate and the other on the surface of secondary sediments. Thick manganese crusts usually form botryoidal structure (Fig. 5−3−1 (1), Photo No. 1), and in rare cases they form stromatolite structure (Fig. 5−3−1 (1), Photo No. 2).

2) Cobble crust (Fig. 5−3−1(2), Photo Nos. 9 to 12)

Cobble crust is defined here as; the whole surface of sample is covered by manganese oxides and the nuclei consist of rock fragments and other material. The long axis of the cobble exceeds 8 cm.

These are formed as manganese crusts cover lava fragments, gravels, floats, talus deposits, and other material separated from the bedrock. Generally, the upper surface of manganese crusts is thicker than the bottom, and the upper surface forms botryoidal structure while the bottom surface forms granule structure. Those which manganese crusts grow thick are often ellipsoidal.

3) Nodule (Fig. 5−3−1 (2), Photo Nos. 13 to 16)

Nodule is defined here as; the whole surface of sample is covered by manganese oxides and the diameter is less than 8 cm.

Nodules generally have a nucleus of rock fragment, but there are some cases that a nucleus does not exist. These are formed under conditions similar to cobble crust, as manganese crusts wholly cover small rock fragments separated from the bedrock. They have spherical, flat, platy and other forms. The surfaces mostly form botryoidal structure, but the structure varies with the thickness of manganese crust and the shape of the nodule.

(2) Layered structure of manganese crusts

In the case where manganese crusts are thick, their sections are divided into two or three layers. Generally they are divided into two layers; an outer layer and an inner layer (Fig. 5–3–1 (2), Photo No. 11). Most thick manganese crusts exceeding 6 cm, however, are divided into three layers and have another layer at the innermost side (Fig. 5–3–1 (1), Photo No. 6). Each layer reflects the age, environment, growth rate, and other factors pertaining to the formation of manganese crusts. In this report, manganese crusts are divided into the following three layers and chemical analysis, various tests, and statistical analysis have been carried out for each layer. The characteristics of each layer observed by the unaided eyes are as follows.

1) Outer layer

This is the surface layer of manganese crusts and the surface generally has botryoidal structure. Usually, it is somewhat compact and its fractured surface is lustrous, but in some cases it is porous and includes brown iron oxide stains. Very thin banded structure is often observed on the section. In the case where manganese crusts are thin, inner and innermost layers are lacking and this layer directly covers the substrate.

This layer corresponds to the part 2 cm thick from the upper surface in Figure 5–3–1 (1) Photo No. 6. The boundary with the inner layer on the lower side is somewhat porous and brown.

2) Inner layer

This is the manganese crust layer on the inner side of the outer layer. It directly covers the substrate in the case where the innermost layer is lacking. The fractured surface is rather rough and there are many pores parallel to the growth direction of the manganese crusts, which often contains unconsolidated muddy material. Brown iron oxide stains occur around the pores. The upper outline of inner layer sometimes shows the same botryoidal cross section as the surface. Generally the boundary with the outer layer is contaminated with brown iron oxides and is relatively clear. The boundary part with the innermost layer is very porous, and the pores are filled with muddy material and contaminated with brown iron oxides.

This layer corresponds to the part 5 cm thick between 2 to 7 cm from the upper surface in Figure 5–3–1 (1) Photo No. 6. Many pores exist and brown iron oxides occur much in the boundary with the innermost layer on the lower side. Near 5cm from the upper side, the pores are filled with pale brown muddy material.

3) Innermost layer

This is the innermost side layer of manganese crusts and directly covers the substrate. This layer is often lacking. It is very compact and hard, and the fractured surface is lustrous. It often has very thin banded structure. The relatively few pores are completely filled with white phosphatized seafloor sediments. The boundary with the inner layer is usually irregular. In some cases, this boundary is smooth with poor ruggedness and the section indicates that the surface were eroded once.

This layer corresponds to the part 2 to 4 cm thick between 7 cm from the upper surface and the substrate in Figure 5–3–1(1) Photo No. 6. There are many white phosphorite network veinlets.

5–2 Results of Seafloor Observation

A TV camera–mounted deep sea towing system (FDC) was used for clarifying the mode of occurrence of the manganese crusts on the seamounts. The FDC track lines were designed to transect the high MBES acoustic pressure zones (where the manganese crusts occur). In other words, the track lines was set either on the margins of the flat summits of the seamounts along the water–depth contour lines, or on the slopes of the seamounts along the steepest slope. The direction of towing was limited to northeastward, eastward, and southeastward by the current and the wind direction, and thus the track lines are mostly on the eastern slope of the seamounts. Observation was done for eight seamounts excluding MS07. It was carried out over a total of 12 track lines, namely one to two lines for each seamount.

Representative seafloor photographs by FDC are shown in Figures 5–2–1 (1), (2), FDC survey results in Appendix Table 1, FDC route maps (plans and sections) and diagrams showing the crust exposure ratios are laid out in Appendix Figures 5 (1) to (12).

The results of the TV observation of each seamount are reported below. The manganese crusts are described in accordance with the classification reported earlier. The manganese crust exposure ratio is the areal extent of the manganese crust exposures (crusts, cobble crusts, nodules) on the seafloor expressed in percentage of the area observed, and it is shown in an average value during one minute observation. The width of the seafloor sweep by TV camera is about 3 m.

(1) MS01

1) Track line 96SMS01FDC01

The track line is located in the northeastern part of the seamount, and the total length is 5.3 miles consisting of 2 miles line in the northwest–southeast direction at the northeastern margin of the flat summit (around 1,300 m deep), and 3.3 miles line extending down northeastward from the flat summit margin to the northeastern lower slope (3,200 m deep). The track line bends at right angles in inverted L-shape.

The track line on the flat summit margin crosses mostly flat areas with small reliefs. The line on the slope has gentle gradient without large relief. The gradient of the upper slope is around 26 degrees and decreases downward to about 9 degrees in the lower part.

Crusts and cobble crusts occur extensively and foraminifera sands are partially predominant on the summit margin in the northwest-southeast trending part of this track line. In crusts and cobble crusts areas, the crust exposure ratio is high, 40 to 90%. On the other hand, the ratio is zero to 10% in areas where the foraminifera sands are predominant. The surface of the crusts shows the botryoidal structure and has ruggedness with small cycle. Cobble crusts occur on the foraminifera

sand or crusts, and some cobble crusts are joined each other or with crusts. Specimens of several cobble crusts joined were dredged at 96SMS01AD11 located on the track line.

On the summit margin in the southwest-northeast trending part of this line, foraminifera sand is predominant, and crusts and cobble crusts are covered by this sand, and some nodules partly occur. At the very end of the summit (around 1,400 m deep), foraminifera sand is extensively distributed and exposures of crusts are almost nil.

As shown in the crust exposure ratios of Appendix Figure 5 (1), the crusts predominant zone and the sand predominant zone are clearly divided on the flat summit. This mode of crust distribution is caused by the micro-topography of the summit. Namely, although the summit is flat as a whole, crusts are exposed where the summit is somewhat sloping, and foraminifera sands are dominant where it is horizontal.

Crusts generally occur at 40 to 100% exposure ratio from the upper to middle slope (1,500 m to 2,300 m deep). The surface of the crusts is botryoidal and irregular. On the lower slope below 2,300 m depth, foraminifera sand becomes predominant and the crust exposure ratio drops to zero to 20%. At below 3,000 m depth crusts are observed, but their surface is not botryoidal and they are probably thin.

Ripple marks occur throughout the surface of the foraminifera sand on the summit and are also often observed on the slopes. Thus it is believed that the foraminifera sand is moving and re-depositing by the bottom current.

The crust exposure ratio tends to decrease downward on the slope. This corresponds to the gradient of the slope, namely the foraminifera sand is not deposited very much over the steeper slope of the upper part and thus the crust exposure ratio is high, while it is thickly deposited on the gentler lower slope. Thus the crust exposure ratio changes by the ease of foraminifera sand

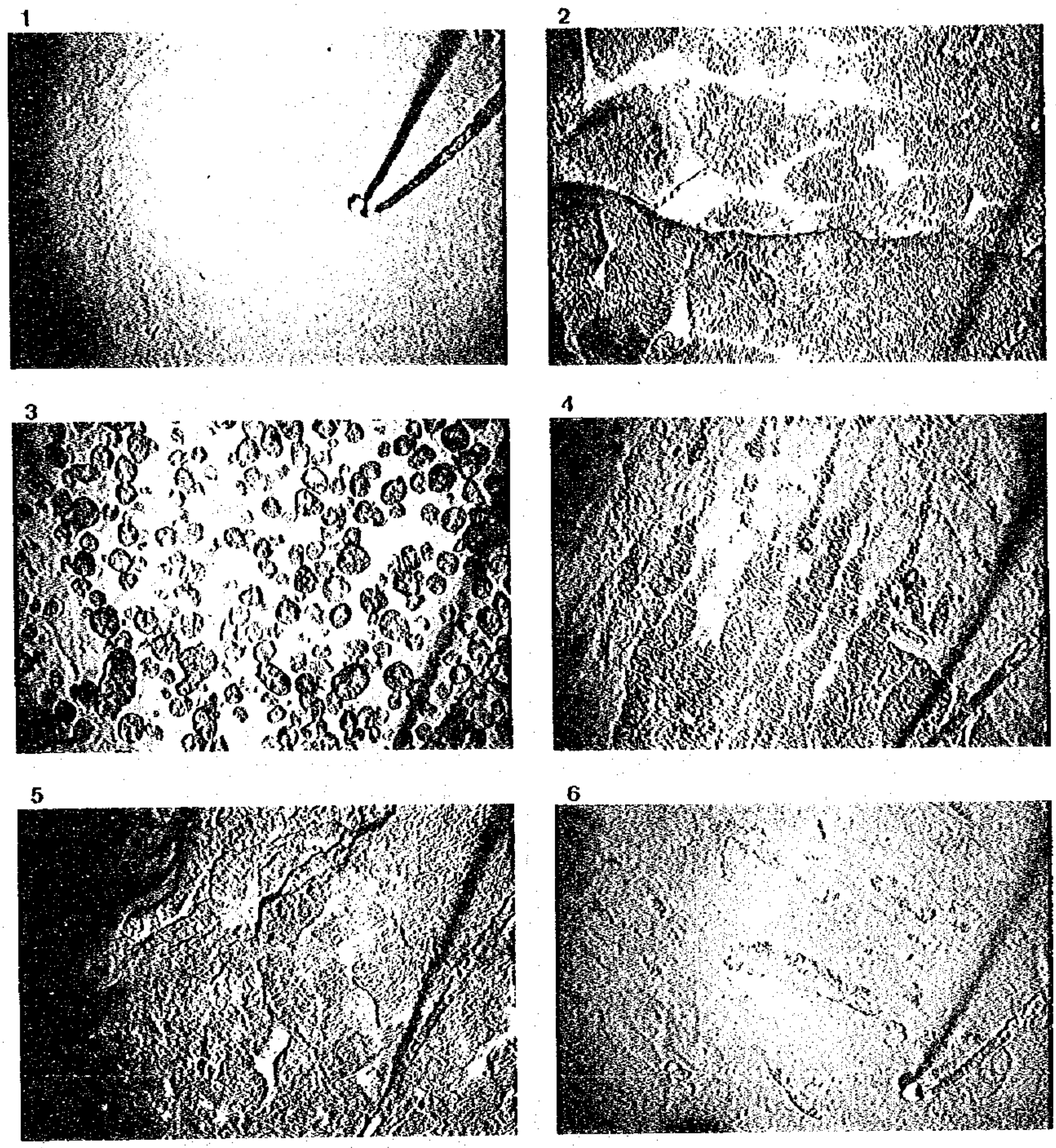

1 96SMS01FDC01 Foraminifera sand and ripple marks
Flat summit margin, Water depth 1,250m, 14° 26.38′ N 161° 03.72′ E

2 96SMS02FDC01 Crust Exposed rate 90%
Flat summit margin, Water depth 1,595m, 14° 02.81′ N 163° 11.49′ E

3 96SMS02FDC01 Cobble crusts and nodules Exposed rate 40%
Flat summit margin, Water depth 1,585m, 14° 03.03′ N 163° 11.87′ E

4 96SMS03FDC01 Foraminifera sand thinly covers crusts Exposed rate 40%
Flat summit margin, Water depth 2,176m, 13° 53.98′ N 164° 06.16′ E

5 96SMS04FDC01 Crusts on a steep slope Exposed rate 90%
Middle part of flank, Water depth 2,029m, 14° 22.92′ N 165° 59.55′ E

6 96SMS04FDC02 Crusts are covered by sand and slightly exposed Exposed rate 10%
Flat summit margin, Water depth 1,112m, 14° 27.81′ N 165° 48.86′ E

Fig. 5-2-1(1) Photographs of FDC seafloor observation

1 2 3 4 5 6

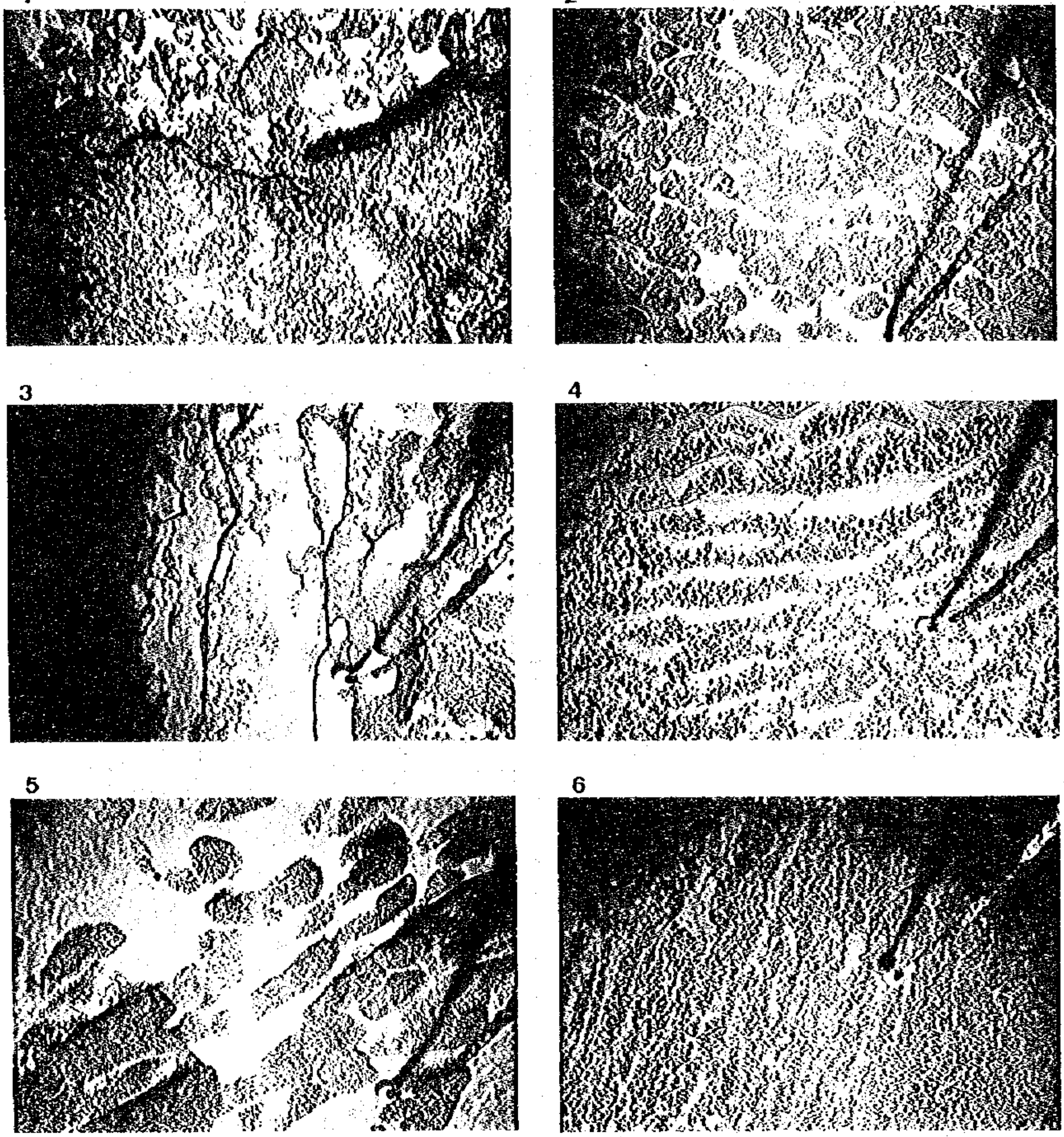

1 96SMS05FDC01 Crusts and cobble crusts Exposed rate 80%
Upper part of flank, Water depth 1,177m, 11° 18.91′ N 171° 04.50′ E
2 96SMS06FDC01 Crusts with pavement structure Exposed rate 70%
Flat summit margin, Water depth 1,818m, 13° 08.50′ N 169° 31.05′ E
3 96SMS06FDC02 Stepped crusts Exposed rate 50%
Flat summit margin, Water depth 1,744m, 13° 09.05′ N 169° 27.59′ E
4 96SMS08FDC01 Nodules are distributed making bands Exposed rate 40%
Upper part of flank, Water depth 2,219m, 14° 01.74′ N 167° 33.55′ E
5 96SMS08FDC02 Crusts with lineation structure Exposed rate 40%
Flat summit margin, Water depth 1,539m, 14° 07.30′ N 167° 23.03′ E
6 96SMS09FDC01 Flat crusts Exposed rate 90%
Middle part of flank, Water depth 2,060m, 16° 31.62′ N 167° 16.70′ E

Fig. 5-2-1(2) Photographs of FDC seafloor observation deposition governed by seafloor topography, bottom current, and other factors.

(2) MS02

1) Track line 96SMS02FDC01

The track line is located at the northeastern part (around 1,600 m water deep) of the flat summit which is elongated in the northeast–southwest direction, and the line extends from the summit center somewhat obliquely to the margin. The length of the line is 3.4 miles and the topography is on the whole flat.

The track line crosses small ridges which extends in the NNW–SSE direction at the western side and the eastern edge. The western ridge is narrow with approximately 40 m relative height, and the slopes are somewhat steep. The eastern ridge has a relative height of approximately 50 m and it is wide with gentle slope. Generally crusts and cobble crusts are predominant on the ridges and their slope, while they are hardly exposed at the depressions and flat land. Ripple marks occur over the surface of the foraminifera sand.

On the eastern ridge at the summit margin, crusts are predominant, and their surface is botryoidal. The crust exposure ratio is very high at 80 to 100%. On the gentle slope of the ridge on the western side, crusts, cobble crusts, and nodules are distributed. The foraminifera sand is dominant where nodules occur and the crust exposure ratio is 10 to 30%. On the other hand, crusts and cobble crusts are predominant where nodules do not occur, and the exposure ratio is 40 to 80%. Nodules occur over the foraminifera sand which in turn cover the crusts.

Cobble crusts and crusts occur on the western ridge and the crust exposure ratio is 30 to 90%. On the eastern slope of this ridge, foraminifera sand is predominant and cobble crusts occur locally. At the central part of the summit which corresponds to the western end of this track line, foraminifera sand occurs extensively without exposure of crusts.

Dredging (96SMS02AD11) at the eastern part of the track line, where nodules are observed to occur, collected only nodules.

(3) MS03

1) Track line 96SMS03FDC01

The track line is located at the eastern part of the seamount, and it transects the eastern margin (2,000 to 2,300 m deep) of the flat summit and extends in the ESE direction down the eastern slope to the middle part (approximately 4,000 m deep). The length is 5.3 miles comprising 2.4 miles on the summit and 2.9 miles on the slope. The topography of the summit is flat without relief, and the slope is monotonous with average grade of 9 degrees.

Foraminifera sand is distributed extensively at the summit margin, and the distribution of the crusts and cobble crusts is intermittent with exposure ratio of zero to 40%. There are ripple marks on the surface of the foraminifera sand throughout the margin.

From the summit margin to the upper slope (2,600 m deep), crusts are predominant and the exposure ratio is high at 50 to 95%. Foraminifera sand is deposited only in depressions and grooves of the crusts. The crust surface is botryoidal. The middle to lower slope (2,600 to 3,000 m deep) is gentler than the upper part and foraminifera sand is widely distributed with very low crust exposure ratio of less than 10%. In the lower slope (3,000 to 4,000 m deep), crusts and cobble crusts occur continuously with local occurrence of nodules. The crust exposure ratio increases downward from 30 to 50% at 3,000 to 3,500 m depth to 50 to 100% at 3,500 to 4,000 m. However, as the crust surface is not botryoidal, the crust is considered to be rather thin coating.

(4) MS04

1) Track line 96SMS04FDC01

The track line is located on the eastern slope of the seamount, and it extends from the eastern margin of the summit (1,100 m deep) down to the lower slope (3,100 m deep). It is 4.9 miles long and the average grade of the slope is approximately 13 degrees.

On the slopes of the seamount, there are many small hills of several hundred meters relative height probably formed by lateral eruption. The track line passes by a hill on the upper slope and crosses two hills at the middle and lower slope. These three hills have relative heights of around 200 m and have steep cliffs on their slopes .

In zones shallower than 1,100 m on the flat summit, crusts are not exposed (exposure ratio zero) and foraminifera sand with ripple marks occurs widely.

On the upper slope (1,100 to 1,600 m deep), crusts and cobble crusts are exposed continuously and the exposure ratio is high, 70 to 100%. The surface of the crusts is botryoidal. From the middle to the lower slope deeper than 1,600 m, foraminifera sand is predominant in most places, but crusts and cobble crusts occur continuously at the two small hills. The exposure ratio on these hills is 40 to 90%, while on the other parts of slopes it is zero to 20% and locally 30 to 60%. In some places of the lower slope, nodules are concentrated. Ripple marks occur on the foraminifera sand surface even in the slopes.

2) Track line 96SMS04FDC02

The track line is located on the northern edge of the flat summit of the seamount, and it transects the summit margin (around 1,100 m deep) in the east–west direction. Both ends of the track line are on the upper slope (around 1,300 m deep). The uppermost slope at the summit margin (around 1,200 m deep) forms a cliff. The summit is flat as a whole, but there are many small reliefs under 20 m relative height.

On the flat summit foraminifera sand is predominantl, and crusts and cobble crusts are distributed intermittently. The surface of the crusts is botryoidal. The crust exposure ratio varies considerably and it tends to increase from the central part of the track line to the flat summit margin. The ratio is mainly less than 10% in the central part of the track line locally increasing to 30 to 70%. The ratio is mainly 30 to 80% on both sides of the line except the slope. Ripple marks generally occur on the surface of the foraminifera sand.

On the upper slope at both ends of the track line, crusts and cobble crusts occur continuously and the exposure ratio is high at 50 to 100%. The crust surface is botryoidal. Foraminifera sand occurs only in the depressions of the crust surface.

(5) MS05

1) Track line 96SMS05FDC01

This is a peaked seamount and this track line transects the summit in the SSW–NNE direction and is 4.3 miles long. The line starts at the upper slope on the southern side (1,500 m deep), climbs the slope north–northeastward, through the summit (900 m deep), and descends the northern slope to 1,600 m depth in the same direction. This is a peaked seamount and the topography is rugged. The slope near the summit is gentle at about 8 degrees.

As the track line is located in the vicinity of the peaked summit, the crust exposure ratio is generally high and the distribution of the foraminifera sand is poor. The surface of the crusts is botryoidal. There are ripple marks on the surface of the foraminifera sand where it occurs locally.

The southern part of the track line is located along the ridge extending south–southwestward and there are many steep cliffs. Crusts and cobble crusts occur continuously and there are some nodules. The crust exposure ratio is 60 to 100% and its average is very high at 80%.

At the summit in the center of the track line, foraminifera sand is predominant and the crust exposure ratio is low at 5 to 30%.

The northern part of the track line crosses obliquely the eastern slope of the seamount in the south, and it lies along the ridge extending north–northeastward in the north. On the eastern slope of the summit, crusts and cobble crusts are continuously distributed immediately below the summit (1,000 to 1,100 m deep) and the crust exposure ratio is 50 to 90%. On the other hand, foraminifera sand is dominant at 1,100 to 1,250 m depth and the crust exposure ratio is zero to 30%. On the ridge at the northern end of the track line (1,200 to 1,600 m deep), crusts and cobble crusts are distributed continuously and the crust exposure ratio is 50 to 100%. Many nodules also occur in this part.

Generally, crusts are dominant on the top and the slope of ridges except the summit and cobble crusts dominant on their base, and nodules are predominant on the flat parts such as the valleys.

2) Track line 96SMS05FDC02

The track line is located at the southeastern slope of the peaked seamount and it descends southeastward from the upper slope (1,300 m deep) to the lower part (3,200 m deep). It is 3.8 miles long. The topographic section show no large relief and is monotonous with an average grade of about 20 degrees.

In the upper part (1,300 to 1,700 m deep), there are many steep cliffs 10 m high and crusts are predominant, but the crust exposure ratio varies considerably from 20 to 100%. The crust surface is botryoidal. At 1,800 to 1,900 m depth corresponding to the foot of a small hill, cobble crusts and nodules are predominant and the crust exposure ratio is 20 to 90%. There are ripple marks on the surface of foraminifera sand.

In the middle to lower slope deeper than 1,900 m, foraminifera sand is predominant and crusts and cobble crusts occur sporadically. In the lower slope (2,900 to 3,100 m deep), there are many stepwise cliffs, and the crust exposure ratio is 20 to 60% in these and locally steep zones. In other parts of this depth, however, the exposure ratio is less than 20% and 0% in many places. At 2,700 to 2,900 m depth, many nodules occur on the foraminifera sand.

(6) MS06

1) Track line 96SMS06FDC01

The track line is located in the northeastern part of the seamount. It starts from the northern edge of the flat summit and extends east−southeastward across the flat summit margin along the edge (1,800 to 1,900 m deep), and descends the eastern slope to its middle part (3,400 m deep). It is 6.9 mile long consisting of 4.6 miles on the flat summit and 2.3 miles on the slope.

The margin of the flat summit has little relief, but 50 to 150 m high cliffs are abundant at the uppermost part of the slope (1,800 to 2,000 m deep). A terrace exists at around 2,400 m water depth on the eastern slope of the seamount, and cliffs are developed immediately below the terrace.

The average grade of the slope is 25 degrees in the upper part and 19 degrees in the middle part.

The western part of the track line transects the projection of the flat summit margin and mainly consists of the uppermost parts of the slope with many cliffs. Crusts and cobble crusts are predominant in the slope and cliffs with the crust exposure ratio of 40 to 90%. On the other hand, foraminifera sand is predominant on the summit and valleys with the exposure ratio of zero to 30%. The crust surface is botryoidal.

At the summit margin in the central part of the track line, foraminifera sand is predominant. Crusts and cobble crusts occur intermittently with exposure ratio of 40 to 80% at both sides of the sand predominant zone where the crust exposure ratio is zero %. Many nodules occur on the eastern part of the summit (1,800 to 1,900 m deep). Ripple marks occur generally on the surface of the foraminifera sand.

On the eastern upper slope (1,900 to 2,300 m deep) on the eastern part of the track line, crusts and cobble crusts occur continuously and the crust exposure ratio ranges from 30 to 100%. The crust surface is botryoidal. On the terrace at 2,400 to 2,500 m depth, foraminifera sand is predominant with cobble crusts and nodules and the crust exposure ratio is 10 to 30%. The middle slope deeper than 2,500 m is dominated by foraminifera sand with intermittent distribution of crusts and cobble crusts, and the crust exposure ratio is zero to 70%.

2) Track line 96SMS06FDC02

The track line is located at the northwestern margin (1,700 to 1900 m deep) of the flat summit and is 5.0 miles long. The summit margin is flat on the whole and some cliffs about 10 m high exist locally.

The western end of the track line (1,900 m deep) is at the uppermost part of the slope and crusts occur continuously with the crust exposure ratio of 40 to 80%. The surface of the crusts is botryoidal.

At the flat summit in the western part of the track line, no crusts are exposed and foraminifera sand is extensively distributed. At the summit in the eastern part of the track line, crusts, cobble crusts, and nodules are exposed at two localities in the vicinity of cliffs and the exposure ratio is 30 to 90%. Except these two sites, however, no crusts are exposed. The surface of the crusts is botryoidal. Ripples marks occur throughout the area on the surface of the foraminifera sand.

As crust–barren part is quite long in this track line, the foraminifera sand is estimated to be considerably thick. The 75 cm long core of foraminifera sand were collected at LC sampling site (96SMS06LC05) in the central part of this line.

This track line was laid on the basis of the SSS survey results, and the correlation between these surveys has been reported in the section of SSS survey.

(7) MS08

1) Track line 96SMS08FDC01

The track line is located at the northeastern part of the seamount, extending from the uppermost slope (1,500 m deep) down northeastward to the lower slope (3,400 m deep). It is 8.6 miles long. Valleys are abundant on the slope of the seamount, and this line is laid nearly along the seafloor valley extending in the southwest–northeast direction. The topographic section along this line shows that relief is poor and the slope is monotonous and gentle with average grade of about 8 degrees.

The western end of the track line (1,500 m deep) is at the outer fringe of the flat summit and only foraminifera sand is distributed with no crust exposures.

On the upper to middle slope (1,600 to 2,400 m deep), there are crust–dominant and foraminifera sand–dominant zones. The crust–dominant zones consist of the uppermost slope (1,600 to 1,700 m deep) and small ridges (1,900 to 2,200 m deep and 2,300 to 2,400 m deep). In these parts, cobbles crusts, crusts, and nodules occur continuously with the crust exposure ratio of 30 to 100%. The crust surface is botryoidal. The foraminifera sand–dominant zones (1,700 to 1900 m and 2,200 to 2,300 m deep) have a lower gradient than the crust–dominant zones. The crust exposure ratio is nil at most places and cobble crusts and nodules locally occur with the ratio of 20 to 50%. There are ripple marks on the sand surface.

The northern part of the track line (deeper than 2,400 m) is located at the bottom of a seafloor valley. On the middle slope (2,600 to 2,700 m deep), crusts, cobble crusts, and nodules are exposed continuously with the crust exposure ratio of 30 to 70%. In other parts, foraminifera sand is dominant with intermittent occurrence of crusts. The crust exposure ratio is mostly 0% and locally 10 to 90%. In the lower slope many nodules occur. Ripple marks occur on the surface of the foraminifera sand.

2) Track line 96SMS08FDC02

The track line is located at the north–central part of the flat summit, and transects the summit in the east–west direction which is elongated in the NNW–SSE direction. The length of the line is 4.2 miles.

The western and central part of the track line (1,540 to 1,600 m deep) are in the central part of the summit and the topography is flat. Foraminifera sand is dominant and the crust exposure ratio is zero % in most of the line, but locally and intermittently cobble crusts and crusts occur with 10 to 70% exposure ratio. There are ripple marks throughout the area over the surface of the foraminifera sand.

The eastern part of the line (1,600 to 1,750 m deep) has a low average grade of 2 degrees. Cobble crusts, nodules, and crusts occur somewhat continuously with the crust exposure ratio of 10 to 70%.

This track line was set on the basis of the SSS survey results, and the correlation of these surveys has been reported in the section of SSS survey.

(8) MS09

1) Track line 96SMS09FDC01

The track line starts from the southeastern–central part of the flat summit transecting the summit margin northeastward, and descends the eastern slope to the middle part (2,700 m deep). It is 5.5 miles long, consisting of 2.5 miles line on the summit and 3.0 miles line on the slope. The summit is topographically flat, but there are large reliefs with the abundance of ridges and small hills on the slope. The average grade of the slope is about 21 degrees on the upper slope and about 17 degrees on the middle part.

Many small hills with several hundred meters height, which are believed to have been formed by lateral eruption, exist on the slope of the seamount. The track line runs through a small ridge in the upper slope and a small hill with 200 m relative height in the middle part.

On the flat summit (less than 1,280 m deep) foraminifera sand is predominant and the crust exposure ratio is zero to 50%. At the western end of the track line in the central part of the summit crusts are not exposed, and in the summit margin they are intermittently exposed. Ripple marks generally occur on the surface of the foraminifera sand.

At the upper slope (1,280 to 2,100 m deep), crusts and cobble crusts occur continuously on the steep uppermost slope and the ridge slope with the high crust exposure ratio of 40 to 100%. Foraminifera sand is predominant in the valleys adjoining the ridges and the exposure ratio is low at zero to 20%. The crust surface is botryoidal. Nodules occur in some parts.

At the middle slope (more than 2,100 m deep), crusts and cobble crusts, and nodules occur continuously on the small hills and their slopes with the exposure ratio of 20 to 50%. On the other hand, foraminifera sand is predominant with zero to 20% exposure ratio on the gentle slope around 2,200 m water depth and on the slope deeper than 2,400 m. The crust surface is botryoidal.